Reply to reviewer 1

Reply to Reviewer 1

The authors would like to thank Reviewer 1 for the helpful comments. We have addressed the issues raised by the reviewer in the following. The review comments are copied in red and our responses are in black normal font and changes in black bold font below.

Ishizawa et al.'s manuscript identify anomalously high GOSAT observations over Japan in summer 2013. They present surface observations (total column and in situ) that seem to corroborate these GOSAT observations and use model simulations to interrogate the source of the methane anomaly. The manuscript is fairly well written. However, I have some serious concerns with the manuscript. In particular, the authors need to account for the seasonal cycle and topography before the data can be used to answer their questions.

2 Major comments:

2.1 Source of the anomaly

The source attribution for this anomaly is severely lacking. The wind patterns do not seem to fit with their discussion. It appears that only the 850 hPa winds in August 2013 would have actually brought high-CH4 airmasses from China (and only to the northern part of Japan). The only thing that seems to really stand out in the rest of the panels is the flow from the Pacific towards southern Japan, why would Saga have a large anomaly from this air? Hysplit runs would be more convincing for showing the sources of the airmasses. As for the CTM results, does the CTM capture the duration of this anomaly? What does a 2012 and 2013 timeseries of XCH4 in the Japan region look like? Does the anomaly show up? What about the simulated surface sites?

Following the reviewer's suggestions and questions, firstly we conducted the backward trajectory calculation to see where air traveled before reaching the two Japanese TCCON sites. These results have been included in the paper **(Fig.12)**. Secondly, the model-observation comparisons of XCH_4 and surface CH_4 time-series have been added in the manuscript **(Figs. 9 and 10)** to show how well the CTM captures the anomaly of

XCH_4.

We employed the STILT modeling system that has been developed based on HYSPLIT coupling with a Lagrangian dispersion component. To see the upstream feature of the summer months, August and September, 100 particles were released from the height of 1500 m of the TCCON sites at every 12:00 noon local time (= 3 UT). The trajectory results have included in Sec 4.1 (**Fig. 12)** after the discussion of wind patterns **(now Fig. 11)**. There are distinct differences in the back trajectory between 2012 and 2013. The trajectory pattern in summer 2012 is very climatological; in August, the wind from the Pacific to the Japan prevails, in September the dominant wind is in a transition from southeasterly wind (from the Pacific) to northwesterly wind (from the continent). On the other hand, in August 2013, the air masses reach the Japanese TCCON sites, after traveling over the coastal side of East China. In September 2013, the westerly wind from the continent is still influential, especially to Saga. These back trajectory results visualize that, the anomalous wind field in summer 2013 brought the CH_4-rich air from China to Japan, resulting in the high XCH_4 observed at the two Japanese TCCON sites and also by GOSAT over Japan.

The CTM simulation results of XCH_4 have been included in the manuscript (**Fig. 9**), compared with the observations. For GOSAT, the modeled XCH_4 values co-located with the GOSAT observations are averaged for comparison. The model simulations are in agreement with the observations, of which correlation coefficients (r) are 0.50-0.72. These correlation coefficient values exceeded the 95% significance level. Furthermore, the model simulations produced the enhancements of XCH_4 in summer 2013. The model was run with cyclo-stationary surface CH_4 fluxes, which are seasonally varying but not inter-annually. Inside the model, only the transport field is varying inter-annually. The model result thus provides supporting evidence that anomalous wind field in 2013 plays a key role in the large XCH_4 event in 2013.

The graphs of the modeled surface CH_4 concentrations for the three Japanese sites, COI, RYO, and YON, have been included (**Fig. 10)**. Though the modeled seasonal amplitude is slightly smaller than the observed, the modeled CH_4 overall captured the observed synoptic variations, as well as the abrupt increase in August 2013 at COI and RYO.

2.2 Real or noise?

Reply to reviewer 1

The authors claim that GOSAT is able to detect synoptic-scale XCH4 enhancements. It's not clear to me that GOSAT was actually able to pick this up and that it's not just an artifact of the analysis. There are other periods in the record that GOSAT seems to do quite poorly compared to TCCON. For example, June/July 2012 in Figure 4 seems to be a ~20 ppb anomaly in TCCON that GOSAT misses. Why is the former anomaly real and the latter just noise? The two sets of TCCON data are the only thing that makes me think this "anomaly" was real and I'm not convinced that GOSAT actually observed it.

More GOSAT XCH_4 retrievals are available in 2013 than 2012. The increase of available retrievals of GOSAT-XCH_4 over Japan improves the correlation between GOSAT and TCCON and also enables GOSAT to detect the 2013 summer anomaly clearly. TCCON-XCH_4 appears to be anomalously low in August 2012 (though the reviewer mentioned June/July 2012). GOSAT-XCH_4 over Japan lowered in August 2012 to the same extent as the TCCON-XCH_4 (see also the **Fig 9**). This study is focused on the anomaly in 2013, using the TCCON XCH_4 as an observational verification. The scope of this study does not mean that the low XCH_4 observed at TCCON sites in summer 2012 is noise.

In addition to the TCCON observations, we have included more model analysis as supporting evidence on the GOSAT-observed anomaly in summer 2013.

Additionally, the authors claim that the modeled XCH4 in August 2013 are lower than 2012 because of these strong zonal winds. However, the GOSAT observations don't seem to support this (Figure 2). Why would the GOSAT observations pick up the Japan high anomaly but not the China low anomaly?

We apologize for the confusion. We need to clarify our explanation of the model result. As the reviewer noticed, the observed GOSAT-XCH_4 in Northeastern China-Korea is not lower in 2013 than in 2012, but rather higher. The wind pattern in 2013 altered the spatial distribution of atmospheric CH_4 over East China. In 2012, the highest concentration appeared over the southeastern China, while in 2013 the hot spot was shifted to the north and also the level of the highest XCH_4 was lower than 2012, as explained below.

First of all, to help distinguish the spatial difference of modeled XCH_4 between 2012 and 2013 in Fig. 7 (**now Fig. 8**), we have changed the color scales. What we emphasize here is how the inter-annually varying wind field alters the spatial distributions of surface CH_4 concentration and XCH_4. In August 2012, the highest XCH_4 appear around the southeastern China, while in August 2013 the highest XCH_4 area shifts northward. Furthermore, the highest XCH_4 level in 2013 is lower than in 2012. Given the same fluxes were used in the model for the both years, these differences between 2012 and 2013 indicate the strong wind carries the CH_4-rich air northward, resulting in less accumulation of CH_4 around the source area in the southeastern China. This tendency is also seen in September. Regarding the XCH_4 in Northeastern China-Korea, the XCH_4 level in 2013 is expected to be higher than that in 2012, as CH_4-rich air masses are transported from the southeastern China more in 2013 than 2012. The time-series of observed GOSAT XCH_4 in Northeastern China-Korea are shown in **Fig. 9**, compared with the modeled XCH_4. The XCH_4 in September 2013 is higher by ~3ppb than in 2012.

2.3 XCH4 in different parts of a region are not directly comparable
Figure 1 shows a simple example of how topography can impact the XCH4. This is why papers like Kort et al. (2014; GRL) computed anomalous methane by removing the bias due to topography. By averaging GOSAT observations over a large region you could be inducing a sampling bias. For example, if you have a higher density of GOSAT observations over Korea in 2012 and then in 2013 you have more observations over Bejing you will almost certainly have a higher regional" XCH4 simply due to topography. This effect can be up to 20 ppb in parts of Japan (near Mt. Fuji).

The topography bias seems to have less impact our analysis. We have included the location maps of GOSAT XCH_4 retrievals we used in this study, including the surface elevation information **(Fig. 3)**. For the entire period 2009-2014 we shown in Fig.2, the surface elevation of XCH_4 over Japan ranges up to 1350m, and ~90% of the data is below 500m. The highest surface elevation of XCH_4 over Japan is ~850 m in 2012/2013. Since we used the NIES L2 CH_4 for General User (GU) which has been applied screening (https://data.gosat.nies.go.jp), there is few retrieval available for the mountainous area in the central Japan (near Mt. Fuji). For Northeastern China-Korea region, the number of observation over Korea was increased in 2013 than 2012. Beijing is located almost at the northwest corner of the target region. There is no significant difference in the observation number around Beijing between 2012 and 2013.

Kort et al. (2014; GRL) analyzed the persisting XCH_4 signal at a higher spatial resolution from the multi-year Satellite data. Our analysis is on the temporal signal on a regional scale, which was detectable at the two TCCON sites, ~1000km apart. The topography bias would be critical when analyzing a signal on a local scale, like an anthropogenic large point source.

Additionally, in 2013 and 2014 you see an increase in GOSAT observations over Japan (bottom panel of Figure 2b). If these happened to be over Tokyo (lower elevation) it could explain part of this "Large XCH4 anomaly". What is the spatial distribution of the GOSAT observations? A figure showing the location of the GOSAT observations would be helpful (maybe observation density).

As we mentioned earlier, the location maps of GOSAT observation have been included in the manuscript. As the reviewer noticed, the number of GOSAT observations over Japan was increased in 2013 and 2014 compared to the previous years. This observation increase did not happen only over Tokyo, but all over the Japan islands. It is due to the observation schedule change by the GOSAT project teams among NIES, JAXA and MOE. In the initial regular schedule, there were fewer soundings over only lands, but most soundings were over oceans or land-ocean mixed locations. The soundings over ocean or mixed locations are difficult to be retrieved. To increase the retrievals over Japan, the observation locations were moved to inland from ocean and mixed locations as much as possible. This observation change was implemented on May 6, 2013.

2.4 Seasonal cycle

I've got a few issues with the treatment of the seasonal cycle:

1. Remove the seasonal cycle in your data. The anomalies seem to be on the order of 20 ppb, this is comparable to the peak-to-peak amplitude of the seasonal cycle. How much of this is seasonal?

Following the reviewer's comment, we have added the time-series removed the mean seasonal cycles **(Fig. 5b**). The amplitude of mean seasonal cycles is around ~20 ppb, comparable with the anomaly we discuss.

2. The seasonal cycle in XCH4 is not necessarily reflective of emissions. The seasonal cycle in the total column does not always follow the seasonal cycle in the emissions (cf. the Bloom et al., 2010 discussion of SCIAMACHY columns and wetland emissions in the Amazon). Changes in stratospheric methane induce higher order harmonics that don't peak when emissions peak. Figure 5 from Saad et al. (2014; AMT) is a nice illustration of this. So statements like, "The summertime high XCH4 must be partially attributed to the seasonal biogenic CH4 emissions from rice paddies and natural wetlands underneath East China and Korea." are not well founded.

Yes, the seasonal cycle in XCH_4 does not only reflect the surface emissions, but also other factors such as, the atmospheric mixing in the troposphere and contribution of stratospheric methane.

We appreciate the reviewer's comment on the seasonality in XCH_4 and emissions. We have made the sentences more moderate, including the reference to Bloom et al. (2010, Science). Firstly, we have changed the sentence from "*The summertime high XCH4 partially attributed to the seasonal biogenic CH_4 emissions from rice paddies and natural wetlands underneath East China and Korea*." to "**The summertime high XCH_4 appear to be influenced by the seasonal biogenic CH_4 emissions from rice paddies and natural wetlands underneath East China and Korea.**" Secondly, we have referred to Bloom et al. (2010, Science), as adding the sentences below, when we discuss the possibility of contribution from the surface emission change in Sec. 4.2. Other possible factors:

Here we discuss two factors. One is the surface emission changes. Though the temporal variations in XCH_4 do not necessarily correlate with the surface emissions (e.g., Bloom et al., 2010), the surface emission change is potential to impact on the change in XCH_4.

Regarding the contribution of stratospheric methane, we have added the paragraph below, refereeing to Saad et al. (2014, AMT):

Another possibility is the contribution of stratospheric methane. Saad et al. (2014) presented the analysis that the stratospheric methane causes short-term fractionations in total column averaged CH4 observed at several TCCON sites.

Reply to reviewer 1

The contribution of stratospheric methane to the anomaly in summer 2013 is supposed to be minor or less influential. Firstly the surface CH4 concentrations at COI and RYO increased in August 2013 when the XCH_4 anomaly occurred, suggesting the major contributor on the anomaly is in the troposphere. Secondly, the order of the stratospheric methane fractionation is smaller than ~3 ppb, which would not be enough to produce the anomaly of an order of ~20 ppb.

3. Figure 7 is presented as "CH4 and XCH4 in August and September 2012 and 2013, with respect to surface CH4 and XCH4 at South Pole". This does not make sense to me. Why would the authors present this as the difference between the Asia and the South Pole? They have different seasonal cycles. CH4 concentrations at 40_N and the South Pole are 6-months out of phase (Northern hemisphere peaks when the Southern hemisphere is at a minimum). This makes interpretation of the plot nearly impossible. Are differences between years due to changes in a different (not shown) hemisphere? Are changes between August and September due to changes in the Southern hemisphere?

To present a spatial distribution with the respect to South Pole is one of typical ways to show the relative spatial distribution. However, to avoid any confusion, we have shown the absolute values of the modeled CH_4 and XCH_4.

3 Minor comments:

Incomplete literature review

The authors don't seem to have cited any of the previous literature on this topic. The last paragraph on page 24997 briefly mentions a couple studies that used in situ observations to estimate methane fluxes but completely neglects the satellite studies (which are the more relevant studies to this work). Examples of relevant studies: Bergamaschi et al. (JGR 2007, JGR 2009, JGR 2013), Fraser et al. (ACP 2013), Monteil et al. (JGR 2013), Wecht et al. (JGR 2014), Kort et al. (GRL 2014), Cressot et al. (ACP 2014), Houweling et al. (ACP 2014), Turner et al. (ACP 2015), and Alexe et al. (ACP 2015) to name a few.

We thank you for pointing out our lack of the literature review. The references of the flux inversion studies using Satellite data have been included, as adding the sentences below in introduction section in the manuscript.

These satellite data have been used for the inversion studies of surface CH4 emissions. Most of the satellite-based inversions are focused on the global-scale estimates (e.g., Bergamaschi et al. 2007; 2009; 2013; Fraser et al., 2013; Moteil et al, 2013; Cressot et al, 2014; Houweling et al., 2014; Alexe et al., 2015). Recently the satellite data have been applied for the flux estimation on a regional- and local-scale at a higher spatial resolution. For example, Wecht et al. (2014) compared the multiple observational constraints including GOSAT and TES to optimize methane emission in California. Turner et al. (2015) estimated North American methane emission at a resolution of up to 50 km×50 km using GOSAT data. Kort et al. (2014) demonstrated that satellite-based observations can quantify localized anthropogenic CH_4 emissions in the Southwest USA

Page 24997, Lines 23: Miller et al. (2013) also use aircraft data.

When categorizing the measurements into two types, ground-based and satellite-based, aircraft measurements belong to ground-based. Therefore, we referred to Miller et al. (2013) there. To describe specifically, we have changed "*ground-based measurements*" to **"ground-based measurements including aircraft and shipboard measurements"**.

Page 24999, Lines 16-17: How are you deducing the large methane sources in China? Bottom-up inventories, EDGAR, something else?

The major CH_4 source in China is anthropogenic. We used the EDGAR v4.2 for anthropogenic emissions, except the rice cultivation. The CH_4 emissions from rice cultivation are from VISIT-CH_4. All the CH_4 emission sources we used in the model run are described in Sec. 3 Model analysis.

Page 25000, Lines 16-18: As I mentioned in the major comment, you can't compare the XCH4 values. There are biases due to topography, for example, that you have not accounted for.

As we answered in our response to the major comment (2.3), the topography biases are not supposed to affect the analysis.

Page 25003, Lines 18-21: Wind patterns don't seem to support this.

As we answered to the major comment (2.1), we have conducted the trajectory analysis, and the results have been included in the manuscript. We keep the wind patterns to help interpret the model simulations and trajectory analysis results.

Page 25004, Line 3: This is very coarse resolution, is this resolution sufficient to resolve these sort of spatial patterns? I'd rather see this plotted without the spatial interpolation, that way we can see the actual model resolution.

We have included the model-observation comparison of time-series as we mentioned earlier in our response to the major comment (2.1).

Page 25005, Line 4-8: However this isn't seen in the GOSAT data. So if this argument were true and GOSAT can pick up the synoptic event then why isn't it seeing this lower XCH4 over China?

Thank you for pointing out the confusion. The summertime XCH_4 over Northeastern China-Korea in 2013 was not lower, but higher than 2012. This statement has been modified to explain clearly, as answered to the major comment earlier. The mode simulation also captures the higher XCH_4 in 2013 (**Fig. 9a**).

Figure 4: Does this have the seasonal cycle removed?

Figure 4 (**now Fig. 5a**) showed the detrended observations which long--term trend components are removed. Now we have added **Fig. 5b**, which are removed mean seasonal cycles from the detrended time-series in **Fig. 5a**.

Figure 8: Shouldn't surface observations in Sept 2013 be lower than average since the air is mostly coming from the Pacific? How is this air coming from China? Especially at Saga.

As we answered to the major comment (2.1), we have conducted the back trajectory analysis and included the results in Sec. 4.1**.** In September 2013, the most of airmasses traveled from China/the continent to Saga (**Fig. 12a**). For Tsukuba, in September 2013 some were from the Pacific, but the air mass from China were more influential than in September 2012.

4 References:

Bloom et al.: Large-scale controls of methanogenesis inferred from methane and gravity spaceborne data. Science 327, 322-5, 2010.

We have added.

Kort et al.: Four corners: The largest US methane anomaly viewed from space. Geophys. Res. Lett. 41, doi:10.1002/2014GL0615053, 2014.

We have added.

Saad et al.: Derivation of tropospheric methane from TCCON CH4 and HF total column observations, Atmos. Meas. Tech., 7, 2907-2918, doi:10.5194/amt-7-2907-2014, 2014.

We have added.

Reply to reviewer 2

Response to Reviewer 2

The authors would like to thank Reviewer 2 for the helpful comments. We have addressed the issues raised by the reviewer in the following. The review comments are copied in red and our responses are in black normal font and our changes in the manuscript in black bold font below.

Major Comments

1) It is unclear how much the GOSAT data itself contributes to this work and whether it is really capturing the signals that are claimed. For example, there are very large discrepancies between GOSAT and TCCON throughout the time period, with GOSAT seemingly having a large amount of variability (noise?). Some quantification of the uncertainty on the GOSAT would make it more convincing that the observed anomalous high values can be trusted.

The main objective of this study is to show how well the GOSAT data capture synaptic-scale variations. For this, we verified the observed enhancement of XCH_4 in the summer of 2013 through the ground-based observations and examined the mechanism using model analysis. As the reviewer commented, GOSAT XCH_4 data have large variability compared with TCCON ground-based observations. That is partially due to larger uncertainty in the retrievals due to many bias factors than the ground-based measurements. This large variability in GOSAT data is a challenge to fully utilize the GOSAT data for flux estimation, even though the GOSAT dramatically expand the spatial coverage of the observation compared with the ground-based measurements. The capability to capture synoptic-scale variations of atmospheric CH_4 is important to improve regional flux estimates because the synoptic-scale variations of atmospheric CH_4 can carry the information on regional surface fluxes. Beside surface fluxes, the atmospheric CH_4 concentrations are highly changeable with the atmospheric transport. Toward improving regional flux estimation, it is essential to observe a synoptic-scale variation of the atmospheric CH_4 and quantify the attribution of such variations. Therefore, in this study, we demonstrate how the GOSAT is capable of detecting a synoptic-scale variation.

Reply to reviewer 2

We modified the introduction in the manuscript to make our objective clear. To verify the GOSAT-observed anomalous high XCH_4, we have added more information on GOSAT observation and analysis results on GOSAT XCH_4, including the back trajectory analysis.

P25001L15/Fig 4. – What is the error on these data points? The GOSAT data seems highly variable and it is difficult to see a correlation until the latter time period. Statements like "data agree overall" need to be quantified.

In Fig. 4 (**now Fig. 5(a)**), both of GOSAT and TCCON values are daily means. The number of GOSAT data per day over the Japan region ranges from 1 to 20, and the average is 3.5 retrievals per day. The mean deviation to daily mean is 9.53 ppb (for >=3 retrievals per day) For TCCON, the average number of retrievals per day is 101.1 per day at Saga and 145 per day at Tsukuba. Moreover, the mean deviation to daily mean is 4.04 ppb at Saga and 5.97 ppb at Tsukuba. To compare the synoptic variations between GOSAT and TCCON, we have included the figure of the time-series removed the mean seasonal cycles from individual de-trended XCH_4 datasets and those monthly means (**Fig. 5(b)**). The correlation coefficients (r) of the monthly means between GOSAT and TCCON Saga, and between GOSAT and TCCON Tsukuba, are 0.81 and 0.61, respectively. These correlation coefficient values exceed the 95% significance level.

2) The use of wind fields in Fig. 8 to argue that this observed enhancement is due to atmospheric transport do not appear to be very convincing. If anything, they would seem to suggest that Saga would primarily be observing clean ocean air. Further analysis/quantification is needed here to make the argument more convincing.

We conducted back trajectory analysis for Saga and Tsukuba. The back trajectory results have been included in Sec. 4.1 in Discussion of the manuscript**. Figure 12** visualizes the air mass reached Saga was traveling inland over East China in August 2013. This supports that the high CH_4 air was transported from China to Saga in August 2013 while the trajectory result for August 2012 is almost climatological; the dominant wind to Saga was from the Pacific, bringing the clean air. In September 2013, most of the air masses to Saga were still from the continent (China), while the air masses in 2012 were mainly from the Pacific.

3) It is unclear what exactly is shown in Figure 7. If it is the enhancement above the South Pole values as it seems, that does not seem to be a useful quantity. It would be of interest to see the actual modelled data here, rather than this enhancement (or have the enhancement calculated in a more meaningful way).

The presentation with respective to the South Pole is one of conventional ways to look at a relative spatial distribution. Responding to the comments from both reviewers and to avoiding further confusion, we have replaced the original Figure 7 with the spatial distribution of actual model output **(Fig. 8).** Also we have included the time-series of modeled XCH_4 for GOSAT and TCOON (**Figs. 9 and 10).**

All the model simulations agree with the observations with the correlation coefficients, r = 0.50-0.72, which exceed the 95% significance level. Furthermore, the modeled XCH_4 capture the observed enhancement of XCH_4 in the summer of 2013.

4) Figure 2 shows a significant increase in the number of GOSAT soundings over Japan in 2013/2014. Presumably this is due to the change in the GOSAT sampling strategy. This should be discussed in more detail, especially regarding any implications this may have that lead to a sampling bias for these latter years. A spatial map of the GOSAT soundings for each year would be of interest and help to indicate whether the enhancement seen in GOSAT is related to the increase in spatial sampling.

As the reviewer noticed, the number of GOSAT soundings over Japan was increased in 2013. We have added the paragraph to explain the change in GOSAT observation over Japan in Sec. 2.1:

The number of GOSAT retrievals over Japan increased in 2013 and 2014, compared with those in the previous years. This increase is due to the change of the observation strategy to increase available GOSAT retrievals over Japan. The initial regular schedule, there were fewer soundings over lands, but most soundings were over oceans or land-ocean mixed locations. The soundings over ocean or mixed locations are difficult to be retrieved. As a result, a few retrievals remained over Japan after screening. Aiming at increasing the retrievals over Japan, the observation locations were moved inland from ocean and mixed

locations as much as possible. The observation strategy change was made as a concerted decision by GOSAT Project terms among the three agencies NIES, JAXA, and MOE. The observation change was implemented on May 6, 2013.

The spatial maps of GOSAT retrievals we used in this study have been included in the manuscript (**Fig. 3**). As seen in **Fig. 3a**, most of the soundings were taken at lower surface elevation; ~80% is below 100m for the entire period. The locations of GOSAT retrievals in August/September, 2012 and 2013 are shown in **Figs. 3b and 3c**. The highest elevation is ~850m in both 2012 and 2013. The number of retrieval over Japan increased in the summer of 2013, around by five-times as the one in the summer of 2012. As far as the China-Korea, there is no significant difference between 2012 and 2013.

5) This manuscript, while generally well-written, would benefit from proof reading by a native English speaker as some sentence structure is grammatically poor and/or confusing. There are too many instances to list each individually but some examples include:
Since 2009, Greenhouse gases Observing SATellite (GOSAT) has been provided column-averaged dry-air mole fractions of atmospheric CH4 (XCH4).
As charactering the observed extreme event
The GOSAT orbiting with three-day recurrence successfully observed the synopticscale XCH4 enhancement in the comparable accuracy to the TCCON data.

The reviewer's comment is helpful to improve our English text. We have rephrased some of the sentences which may confuse the readers, including those listed above.

6) The manuscript would benefit from further explanation on where this work sits in the context of other recent GOSAT/CH4 studies. As mentioned by the other reviewer, the literature review here is sorely lacking and would add important context to this work.

As mentioned in our response earlier, our objective is to examine the high XCH_4 anomaly and to demonstrate the capability of GOSAT to capture synoptic-scale events, which is required to improve the regional flux estimates. We have added the sentences below in introduction of the manuscript to explain the background and the implication of this study:

The capability to capture synoptic-scale variations of atmospheric CH_4 leads to better regional flux estimation because the synoptic-scale variations of atmospheric CH_4 can carry the information on regional surface fluxes. On the other hand, the atmospheric CH_4 concentrations are highly changeable with the atmospheric transport as well as surface fluxes. Toward improving regional flux estimation, it is essential to observe better a synoptic-scale variation of the atmospheric CH_4 and quantify the attribution of such variations.

As both reviewers pointed out, our original manuscript is in a lack of relevant references, especially to the satellite-based inversion. We have added the references to the inversion studies using satellite data in the introduction section, mentioning the recent satellite studies focusing on a regional- and local-scale at the high spatial resolution.

Minor Comments/Technical Corrections

P25001L4 – Please include the version number for the TCCON data. TCCON data now also has a DOI and should be cited accordingly.

TCCON data started having DOI from GGG2014. We used GGG2012. This case we understand the references for the data is sufficient.

P25008L19 - CCON data -> TCCON data

We have corrected.

Large XCH_4 anomaly in summer 2013 over Northeast Asia observed by GOSAT

M. Ishizawa[1], O. Uchino[1], I. Morino[1], M. Inoue[1*], Y. Yoshida[1], K. Mabuchi[1], T. Shirai[1], Y. Tohjima[1], S. Maksyutov[1], H. Ohyama[2], S. Kawakami[3] and A. Takizawa[4]

[1]{National Institute for Environmental Studies, Tsukuba, Japan}

[2]{Solar-Terrestrial Environmental Laboratory, Nagoya University, Nagoya, Japan}

[3]{Japan Aerospace Exploration Agency, Tsukuba, Japan}

[4]{Japan Meteorological Agency, Tokyo, Japan}

[*]{now at: Akita Prefectural University, Akita, Japan}

Correspondence to: M. Ishizawa (ishizawa.misa@nies.go.jp)

Abstract

Extremely high levels of column-averaged dry-air mole fractions of atmospheric methane (XCH_4) were detected in August and September 2013 over Northeast Asia (~20 ppb above the averaged summertime XCH_4 over 2009-2012, after removing a long-term trend), as being retrieved from the Short-Wavelength InfraRed (SWIR) spectral data observed with the Thermal And Near-infrared Sensor for carbon Observation - Fourier Transform Spectrometer (TANSO-FTS) onboard Greenhouse Gases Observing Satellite (GOSAT). Similar enhancements of XCH_4 were also observed by the ground-based measurements at two Total Carbon Column Observing Network (TCCON) sites in Japan.

The analysis of surface CH_4 concentrations observed at three monitoring sites around the Japan islands suggest that the extreme increase of XCH_4 has occurred in a limited area. The model analysis was conducted to investigate this anomalously high XCH_4 event, using an atmospheric transport model. The results indicate that the extreme

increase of XCH_4 is attributed to the anomalous atmospheric pressure pattern over East Asia during the summer of 2013, which effectively transported the CH_4-rich air to Japan from the strong CH_4 source areas in East China. The two Japanese TCCON sites, ~1,000 km east-west apart each other, coincidentally located along the substantially CH_4-rich air flow from East China. The GOSAT orbiting with three-day recurrence successfully observed the synoptic-scale XCH_4 enhancement in the comparable accuracy to the TCCON data. This analysis demonstrates the capability of GOSAT to monitor an XCH_4 event on a synoptic scale. We anticipate that the synoptic information of XCH_4 from GOSAT data contributes to improve our understanding of regional carbon cycle and the regional flux estimation.

1 Introduction

Atmospheric methane (CH_4) is the second important anthropogenic greenhouse gas after carbon dioxide (CO_2), contributing about 20 % of the total radiative forcing from the major well-mixed greenhouse gases (Forster et al., 2007). Methane has multiple natural and anthropogenic sources in the Earth's surface while being mainly removed through reaction with hydroxyl radical (OH) in the troposphere and by photolysis in the stratosphere. The atmospheric CH_4 level has more than doubled since the onset of the industrial revolution in the 18th century (Etheridge et al., 1998). Its growth rate has been considerably variable over the past few decades (Dlugokencky et al., 2009). On a global scale, the causes of recent changes in the CH_4 growth rate remain unknown (e.g. Kirschke et al., 2013; Dlugokencky et al., 2009), and on a regional scale, significant discrepancies have been found in the emission estimates between bottom-up and top-down approaches (e.g. Miller et al., 2013). On the other hand, given the larger radiative forcing than carbon dioxide, it has been argued that reducing anthropogenic CH_4 emission might be a mitigation of possible severe impact of global warming (e.g. Hansen and Sato, 2004). Therefore, to elucidate the drivers of changes in atmospheric CH_4 concentrations and to quantify the regional source distributions are challenging tasks.

The temporal variations of observed atmospheric CH_4 are complicated due to various sources on the Earth surface, interactions between the emission sources and the atmospheric transport, and removal in the atmosphere. To improve the regional CH_4 flux estimates on the Earth surface, it is needed to better understand the relative contribution of atmospheric transport to the observed variations of atmospheric CH_4.

In the past decades, the investigations of the spatiotemporal variability in atmospheric CH_4 concentrations and the inverse modeling estimates of surface CH_4 flux estimates had been mainly based on the ground-based measurements including aircraft and shipboard measurements (e.g. Bousquet et al., 2006; Bergamaschi et al., 2010; Miller et al., 2013). However, the current ground-based measurements of CH_4 are still sparse. In the recent years, the measurements from the satellites have been providing the large spatial and temporal coverage to help better understand the variations of atmospheric CH_4. ~~Since 2009,~~ Greenhouse gases Observing SATellite (GOSAT) was launched in January 2009~~, has been~~, providing column-averaged dry-air mole fractions of atmospheric CH_4 (XCH_4) that are retrieved from Short-Wavelength InfraRed (SWIR) solar spectra observed onboard Thermal And Near infrared Sensor for carbon Observation - Fourier Transform Spectrometer (TANSO-FTS) instrument (Yokota et al., 2009; Yoshida et al., 2013). The GOSAT TANSO-FTS aims at providing measurements of atmospheric CH_4 concentrations in three-month averages with an accuracy of better than 2 % at 100-1,000 km spatial resolution (Kuze et al., 2009). GOSAT XCH_4 is preceded by the several previous and on-going satellite projects, for example, the Infrared Atmospheric Sounding Interferometer (IASI, Crevoisier et al., 2009), and the Tropospheric Emission Spectrometer (TES, Wecht et al., 2012) and the SCanning Imaging Absorption spectroMeter for Atmospheric CHartographY (SCIAMACHY, Schneising et al., 2011). Among them, XCH_4 retrievals from SCIAMACHY instrument onboard ENVISAT launched in 2003 was pioneering, but the communication with ENVISAT was lost in April 2012. T~~he GOSAT TANSO-FTS aims at providing measurements of atmospheric CH_4 concentrations in three-month averages with an accuracy of higher than 2 % at 100-1,000 km spatial resolution (Kuze et al., 2009).~~ These satellite data have been used for the inversion studies of surface CH_4 emissions. Most of the satellite-based inversions are focused on the global-scale estimates (e.g., Bergamaschi et al. 2007; 2009; 2013; Fraser et al., 2013; Moteil et al, 2013; Cressot et al, 2014; Houweling et al., 2014; Alexe et al., 2015). Recently the satellite data have been applied for the flux estimation on a regional-and local-scale at a higher spatial resolution. For example, Wecht et al. (2014) compared the multiple observational constraints including GOSAT and TES to optimize methane emission in California. Turner et al. (2015) estimated North American methane emission at a resolution of up to 50 km×50 km using GOSAT data. Kort et al. (2014) demonstrated that satellite-based observations can quantify localized anthropogenic CH_4 emissions in the Southwest USA

Here, we report the extremely high XCH_4 event observed by GOSAT in August and September 2013 over Northeast Asia. Similar high XCH_4 event were also detected by the ground-based measurements at the two Japanese Total Carbon Column Observing Network (TCCON) sites in Tsukuba and Saga. Given the spacing and temporal frequency (three-day recurrence) of GOSAT sampling, along with possible retrieval biases of XCH_4 retrievals, it is interesting that the GOSAT detected the synoptic-scale variation of XCH_4 that is coherent with the ground-based measurements. This GOSAT-detected XCH_4 event suggests the potential of GOSAT XCH_4 analysis in higher temporal and spatial resolution. The capability to capture synoptic-scale variations of atmospheric CH_4 leads to better regional flux estimation because the synoptic-scale variations of atmospheric CH_4 can carry the information on regional surface fluxes. On the other hand, the atmospheric CH_4 concentrations are highly changeable with the atmospheric transport as well as surface fluxes. Toward improving regional flux estimation, it is essential to observe better a synoptic-scale variation of the atmospheric CH_4 and quantify the attribution of such variations.

In this study, ~~in order to demonstrate how the GOSAT is capable to detect a synoptic-scale variation,~~ we analyse the extremely high XCH_4 observed by GOSAT in the summer of 2013 and investigate the attributions of such a significant increase of XCH_4. ~~As charactering the observed extreme event of atmospheric CH_4 in terms of spatial extent and temporal duration,~~ We discuss how capable GOSAT XCH_4 is to monitor synoptic-scale XCH_4 variations.

2 Observations

2.1 GOSAT XCH_4

GOSAT is a joint project of the Japanese Ministry of the Environment (MOE), the National Institute for Environmental Studies (NIES) and the Japan Aerospace Exploration Agency (JAXA) to monitor the global distribution of atmospheric CO_2 and CH_4 from space (Yokota et al., 2009). The retrieved XCH_4, as a part of NIES GOSAT Level 2 (L2) product (v02.xx), has been reported to have a mean bias of -5.9 ppb and mean standard deviation of 12.6 ppb against the XCH_4 at selected TCCON sites (Yoshida et al., 2013). In this study, we analysed NIES GOSAT L2 XCH_4 (v02.21) without any bias correction. The description of the latest updated retrieval procedures and the auxiliary information can be found at GOSAT User Interface Gateway (https://data.gosat.nies.go.jp).

We analysed GOSAT XCH_4 over two regions in Northeast Asia separately (Fig. 1). One is over northeastern China-Korea (115˚E-130˚E, 30˚N-40˚N), and the other is over Japan (130˚E-145˚E, 30˚N-40˚N). The northeastern China-Korea region covers highly populated and industrialized areas with large anthropogenic CH_4 sources in the Eurasia continent. The Japan region has small CH_4 sources, but located downwind of the continental CH_4 emissions. Time-series of XCH_4 data from June 2009 to March 2014 over the two regions with monthly means are shown in Fig. 2. It is noted that we used only the XCH_4 over land to minimize possible errors depending on sounding observation mode (Fig. 3). In fact, since a few soundings over ocean around East Asia were retrieved, removed XCH_4 data through this criterion are less than 5% of the total. A long-term trend component in each XCH_4 dataset derived through a digital filtering of two-year cutoff period (Nakazawa et al., 1997) is also plotted in Fig. 2. To focus the seasonal variations, the trend components were removed, and the detrended XCH_4 time-series are further analysed.

The GOSAT XCH_4 retrievals over Northeastern China-Korea have clear seasonality with high peaks in summer and low peaks in winter. The summertime high XCH_4 ~~must be~~ appear to be influenced ~~partially attributed to~~ by the seasonal biogenic

CH_4 emissions from rice paddies and natural wetlands underneath in East China and Korea. The summer peak in 2013 was more prominent than the preceding two years, 2011 and 2012. Also, the summertime XCH_4 retrievals over Northeastern China-Korea in 2009 and 2010 were relatively high while no significantly high XCH_4 was observed over Japan. Since there is a limited number of retrieval available over Japan for the first two years of the GOSAT operation, it is difficult to discuss the XCH_4 difference over the two regions for 2009 and 2010. We thus leave this topic for a future investigation.

The seasonality of the GOSAT XCH_4 retrieval over Japan is overall similar to Northeastern China-Korea. Although the seasonal cycle varies largely year-to-year, XCH_4 retrievals of August and September in 2013 were outstandingly high. Japan is located downwind of strong anthropogenic and natural biogenic CH_4 emissions in the continent, and then the signals of the continental CH_4 emissions are lowered as the air is transported. However, it is noticeable that, in the summer of 2013, the XCH_4 retrievals over both Japan and Northeastern China-Korea regions reached the almost same high levels. This comparable XCH_4 levels in the two regions indicates there was a mechanism of fast atmospheric transport in 2013 to bring CH_4-rich air to Japan with less diffusion than the preceding years.

The number of GOSAT retrievals over Japan increased in 2013 and 2014, compared with those in the previous years. This increase is due to the change of the observation strategy to increase available GOSAT retrievals over Japan. The initial regular schedule, there were fewer soundings over lands, but most soundings were over oceans or land-ocean mixed locations. The soundings over ocean or mixed locations are difficult to be retrieved. As a result, a few retrievals remained over Japan after screening. Aiming at increasing the retrievals over Japan, the observation locations were moved inland from ocean and mixed locations as much as possible. The observation strategy change was made as a concerted decision by GOSAT Project terms among the three agencies NIES, JAXA, and MOE. This observation change was implemented on May 6, 2013.

The spatial maps of GOSAT retrievals we used in this study are shown in Fig. 3. As seen in Fig. 3a, most of the soundings were taken at lower surface elevation; more than 80% is below 100m, 95% is below 500m. The spatial maps of the retrievals in August and September in 2012 and 2013 are shown in Fig. 3b and Fig. 3c, respectively. Obviously the number of retrievals over Japan was dramatically increased in 2013, compared with 2012. As far as the China-Korea, there is no significant difference between 2012 and 2013.

2.2 TCCON XCH_4

Inside the Japan region of this study, ground-based XCH_4 measurements have been conducted at two TCCON sites, Saga (33.24˚N, 130.29˚E) and Tsukuba (36.05˚N, 140.12˚E) as shown in Fig. 1. TCCON is a worldwide network of ground-based high-resolution FTSs, which record spectra of the direct sunlight in the near-infrared, and provides accurate and precise column-averaged dry-mole fractions of atmospheric constituents including CO_2, CH_4, N_2O, HF, CO, H_2O, and HDO retrieved from these spectra absorbed by them (Wunch et al., 2011). The TCCON XCH_4 measurements have an estimated uncertainty of 7 ppb (2σ) (Wunch et al., 2010). TCCON data play a critical role in the validation of space-based measurements. The Saga TCCON site is in Kyushu Island, operated by JAXA since June, 2011. The Tsukuba TCCON site is located ~50 km north of Tokyo in the Japan main island, operated by NIES since 2009. These two Japanese TCCON sites are apart ~1,000 km longitudinally. In this study, we use the TCCON data processed by GGG 2012.

Figure ~~3~~4shows XCH_4 retrievals at Saga and Tsukuba TCCON sites during the period for 2011 to 2014. We processed the both TCCON XCH_4 time-series in the same manner with the GOSAT XCH_4 to obtain the long-term trends that are shown in blue lines in Fig. ~~3~~4. It is interesting that, before the summer 2013, XCH_4 retrievals at Tsukuba overall are lower than at Saga. Since Saga is located closer to the continent than Tsukuba, Saga is considered to be influenced by the continental anthropogenic CH_4 emissions more strongly than Tsukuba. In the summer of 2013, extremely high XCH_4 retrievals both at Saga and Tsukuba were observed, reaching almost a same level. This XCH_4 enhancement observed at the ground-based TCCON sites is coincident with the high XCH_4 observed by GOSAT, and strongly supports our speculation that the CH_4 rich air was transported quickly from the continent to Japan for this period.

To focus on the seasonal and synoptic variations, we compared the detrended XCH_4 time-series from GOSAT over Japan and the two Japanese TCCON sites. Figure ~~4~~ 5a shows that all the detrended XCH_4 data are overall in phase of seasonal cycle with seasonal amplitude of ~20 ppb. ~~agree overall with each other in the timing of seasonal cycle.~~ Compared with TCCON XCH_4, GOSAT XCH_4 shows large short-term variability, ~~but has small seasonal amplitude of ~10 ppb. In 2012, both GOSAT XCH_4 and TCCON XCH_4 at the two sites increased together by ~10 ppb while the increase of GOSAT XCH_4 was not clearly seen show no clear tendency in August, while they as a whole appear to be upward in September.~~ In 2013, both GOSAT and TCCON XCH_4 together rapidly increased in August and remained high in September. In 2012, both GOSAT XCH_4 and TCCON XCH_4 ~~at the two sites increased together by ~10 ppb while the increase of GOSAT XCH_4 was not clearly seen~~ show no clear tendency in August, and all of them appear to be upward in September. On average, the XCH_4 level of GOSAT over Japan in August and September 2013 is higher by ~15 ppb than 2012. The XCH_4 levels of both TCCON sites in 2013 are higher by ~20 ppb than 2012. These enhancements of XCH_4 are comparable to their seasonal amplitude.

To examine further how the synoptic variability of GOSAT is correlated with TCCON, we removed the mean seasonal cycles from the detrended XCH_4 time-series and took the monthly means (Fig. 5b). Except the months when the retrievals are available for less than two days, the correlation coefficients (r) of the monthly means between GOSAT and TCCON at Saga, and between GOSAT and TCCON at Tsukuba, are 0.81 and 0.61, respectively. These correlation coefficient values exceed the 95% significance level. Despite the large short-term variability, the synoptic variability of GOSAT over Japan is overall correlated with the TCCON XCH_4 at two Japanese sites. The enhancement of XCH_4 in the summer of 2013 is consistent among GOSAT and TCCON. If the period is limited to May–December 2013, when the number of GOSAT XCH_4 retrievals was increased due to the observation strategy change mentioned earlier, the correlation coefficients (r) between GOSAT and TCCON are improved to be 0.91 with Saga and 0.96 with Tsukuba. This implies that the increase in the observations over Japan improves the capability of GOSAT to detect synoptic variability in XCH_4.

2.3 Ground-based surface CH_4 concentrations

In order to see the relationship between the surface CH_4 concentration and the enhancement of GOSAT XCH_4 over Japan, we analyzed the surface CH_4 concentrations observed at three ground-based monitoring stations in Japan, Cape Ochi-ishi (COI, 43.16˚N, 145.49˚E), Ryori (RYO, 39.03˚N, 141.82˚E), and Yonagunijima (YON, 24.47˚N, 123.02˚E). These site locations are shown in Fig. 1. At all the stations, continuous measurements of atmospheric CH_4 are conducted. Cape Ochi-ishi (COI) is a station operated by NIES, which is located at the east tip of Hokkaido island (Tohjima et al., 2002). Ryori (RYO) is located inside the Japan region defined in this study, where the monitoring of surface greenhouse gas concentrations has been conducted by the Japan Meteorological Agency (JMA) as a part of the Global Atmospheric Watch (GAW) program of the World Meteorological Observation (WMO). RYO is on the west coast of the Japan main island, about 300 km north of Tsukuba and far away from direct influences of residential and industrial pollutants. Yonagunijima (YON) is also one of JMA-operated GAW stations, which is located far south of the Japan main island and east of ~110 km of Taiwan. The details on RYO and YON are provided on the web page of WMO GAW World Data Centre for Greenhouse Gases (WDCGG) (http://ds.data.jma.go.jp/gmd/wdcgg/introduction.html).

The time-series of surface CH_4 concentrations at the three ground-based stations are shown in ~~Fig. 5~~ Fig. 6, with their monthly means and long-term trends. Here we analyzed the afternoon mean CH_4 (averaged hourly CH_4 over 12:00 - 15:00 local time) from the respective data sets, assuming that the afternoon values are large-scale representative. The observed CH_4 concentrations at all the sites show similar seasonal cycles in timing. Seasonally the CH_4 values are low in July and August, and high in winter to spring. In the winter, the westerly wind prevails and transports the CH_4-rich air from the continent (mainly anthropogenic CH_4 emitted in East China) to Japan, causing the rise of CH_4 concentrations. In the summer, the southeasterly wind is dominant, bringing clean air to Japan from the Pacific Ocean, where is no major CH_4 source, so that the surface CH_4 concentrations become low.

In the summer of 2013, unseasonably high CH_4 concentrations were observed at RYO with a sharp increase in the middle of August. The CH_4 concentrations at COI started increasing earlier from its summer minimum than the previous year, 2012. At YON, no significant CH_4 enhancement was seen in 2013 compared with the previous years. Since no similar CH_4 change to RYO and COI was observed at YON, the farthest southwestern island of Japan, this significant CH_4 enhancement event appears to be spatially limited in the area around Japan main island and Hokkaido island. To further examine the summer increase of surface CH_4 concentrations, we compared the detrended CH_4 at RYO and COI for the two years of 2012 and 2013 (Fig. ~~6~~ 7). The timing and amplitude of seasonal cycles at RYO and COI overall agree well with each other, except for the summer of 2013. In August and September of 2013, the temporal variations of CH_4 at RYO and COI are different from those in the previous year 2012 when the CH_4 concentrations were low over the summertime and started rising at the end of September. In August 2013, the abrupt CH_4 increase by ~100 ppb was observed at RYO, followed by COI with ~1 week delay. In September, the CH_4 at both sites lowered but stayed in the higher level than 2012. Given that the fact the major CH_4 sources in East China, the sudden large increase of CH_4 in August 2013 is probably caused by unseasonal transport of CH_4-rich air from the continent to Japan though normally in August the wind with CH_4-low air from the Pacific Ocean is prevailing over Japan.

3 Model analysis

The observational data analysis suggested that the atmospheric transport would be a key factor of the extreme enhancement event of XCH_4 and surface CH_4 concentrations in the summer of 2013 over Japan. To investigate how the inter-annually varying atmospheric transport plays the role in the enhancement of XCH_4 and surface CH_4, we conducted a forward model simulation using the global atmospheric transport model of National Institute for Environmental Studies (NIES-TM) version 8.1i.

The NIES-TM has a horizontal resolution of 2.5°×2.5° with 32 vertical layers (Belikov et al., 2013). The global wind fields used in this study were obtained from the JMA Climate Data Assimilation System (JCDAS) (Onogi et al., 2007). The planetary boundary layer height data are obtained from the European Centre for Medium-Range Weather Forecasts (ECMWF) Interim Reanalysis dataset (Dee et al., 2011). In order to examine the impact of time-varying atmospheric transport on the seasonal cycles of atmospheric CH_4 and XCH_4 fields, the CH_4 emissions averaged over 2009-2010 were repeatedly used during the entire model simulation period for 2009-2013. The CH_4 emissions comprise anthropogenic fluxes and natural fluxes. The anthropogenic fluxes are from the Emissions Database for Global Atmospheric Research (EDGAR) inventory, v4.2 FT2010 (http://edgar.jrc.ec.europa.eu/). The natural CH_4 fluxes are biomass burning from Global Fire Emissions Database (GFED) v3.1 (van der Werf et al., 2010), wetland, rice paddy emissions and soil sinks from the Vegetation Integrative Simulator for Trace gases (VISIT) (Ito and Inatomi, 2012), and termites (Fung et al., 1991). Except the termites CH4 emission, all the natural fluxes are seasonal. We used the modeled methane loss and climatological OH fields provided for a model inter-comparison project "TransCom-CH_4" (Patra et al., 2011).

Figure ~~7~~ 8 shows the simulated surface CH_4 concentration and XCH_4 fields for August and September in 2012 and 2013. ~~Both fields are plotted with respect to the surface CH_4 concentration and XCH_4 at the South Pole to examine the inter-annual variations, removing the long-term trends in the model simulations.~~ As a common feature, the high levels of XCH_4 and surface CH_4 are found over East China, reflecting the spatial distribution of the strong anthropogenic emissions around Beijing and Shanghai and biogenic CH_4 sources from rice cultivation in the southeastern China.

Different patterns are found in the XCH_4 and surface CH_4 fields between 2012 and 2013. In August 2012, both levels of XCH_4 and surface CH_4 over Japan are as low as those over the Pacific oceans. In August 2013, higher concentrations of surface CH_4 extended from the northeastern China and the Korean peninsula to the Japan islands. The surface CH_4 concentration level in 2013 over Japan is increased by 40-60 ppb from the level in 2012. The XCH_4 values over Japan are also enhanced by ~~~30~~ 20 ppb while the XCH_4 values over the southeastern ~~East~~ China ~~coast~~ are lowered compared to the 2012 level. ~~These simulated enhancements of XCH_4 and CH_4 concentration over Japan are comparable to the observations (Figs. 4 and 6).~~ The lower concentrations in August 2013 over ~~East~~ the southeastern China than 2012 indicate that the northward wind ~~toward the~~

north along the coast was so fast that CH_4 was not much accumulated over the CH_4 source area in the southeastern China, but transported away to the north. As a result, the areas of the highest levels of CH4 and XCH4 shifted to the northeast, from the southeast China. In September 2013, XCH_4 level over the southeastern China is higher than August, but still lower than the level of September 2012. Also the XCH_4 over Japan remains higher level than that of 2012. The surface CH_4 concentration pattern in September 2013 is almost similar to the one in 2012, but slightly higher values are found over Japan. ~~This model exercise indicates the inter-annual variation of atmospheric transport would be the key to the large anomalies of XCH_4 and CH_4 concentrations over Japan in the summer of 2013.~~

Figure 9 shows the time-series of modeled XCH_4 for GOSAT and TCCON, compared with the observations. For GOSAT, the modeled XCH_4 co-located with the GOSAT observations are sampled and averaged for comparison. The modeled XCH_4 produce the enhancement in summer 2013, in phase with the observations (Fig. 9). Overall the temporal variations of modeled XCH_4 are correlated with the observations (r = 0.50-0.72). These correlation coefficient values exceeded the 95% significance level. The seasonal cycles of modeled XCH_4 for GOSAT and TCCON are in good agreement with the observations, while the modeled GOSAT XCH_4 show less short-term variability then the observations. The modeled surface CH_4 concentrations for the three Japanese sites, COI, RYO, and YON, are shown in Fig. 10. Though the modeled seasonal amplitude is slightly smaller than the observed, the modeled CH_4 overall capture the observed synoptic variations, as well as the abrupt increase in August 2013 at COI and RYO. The model was run with cyclo-stationary surface CH_4 fluxes, which are seasonally varying but not inter-annually. Inside the model, only the transport field is varying inter-annually. The model-observation comparison thus provides supporting evidence that anomalous wind field in 2013 plays a key role in the large XCH_4 event in 2013.

4 Discussions

4.1 Characteristics of Atmospheric Circulation in the summer of 2013

Forward modeling gives us insights into the contribution of atmospheric transport on the enhancement of XCH_4 and surface CH_4 concentration in the summer of 2013 over Japan. Here we examine the 2013 summertime atmospheric transport over the northeastern Asia.

Japan's summer climate is governed by the Pacific High (a lower-level high-pressure system) and the Tibetan High (an upper-level high-pressure system). These pressure systems were reported to have been enhanced during July and August 2013 (Tokyo Climate Center News No.34 Autumn 2013, available at http://ds.data.jma.go.jp/tcc/tcc/news). The Pacific High continued to expand westward and largely developed over the western part of Japanese islands including Okinawa. The Tibetan High expanded to the Japan main island in line with the northward meandering of upper-level westerly winds (the subtropical jet stream). The enhanced atmospheric transport from East China to Japan was probably attributed to those anomalously developed high-pressure systems.

To see how the 2013 summertime atmospheric transport differs from the mean transport pattern, Fig. ~~8~~11 shows the wind fields at the surface and at 850 hPa pressure level, from the JCDAS wind fields of August and September in 2013 over East Asia, compared with those of the mean wind fields for the five years of 2009-2013.

At the surface level (Fig. ~~8~~11a), the mean wind field clearly shows that, in August the southeasterly wind from the Pacific Ocean prevails ~~as a result of~~ due to the development of the Pacific High. In September the wind from the continent to Japan start blowing as the Pacific High is retiring. In August 2013, as the Pacific High expanded westward, the air moved northward along the coast of China, turned around the Korean Peninsula, and flowed to Japan. This wind pattern suggests that the CH_4-rich air was transported from East China to Japan in 2013, while the clean air is normally transported from the Pacific Ocean. In September 2013, over the Pacific Ocean, south of the Japan main island, easterly wind was still stronger than the normal, but the wind pattern over Japan was almost back to the normal, which can be characterized as a weak convergence of westerly wind from the continent and easterly wind from the Pacific Ocean. This nearly normal wind pattern over northern Japan would lower the CH_4 concentrations at the surface level as observed at RYO and COI.

At the 850 hPa level (Fig. ~~8~~11b), it is notable that, in August 2013 the air moved over the East China along the coast and turned around the Korean peninsula sharply to the Japan islands. The anomalous westerly winds were stronger in the upper levels than near the surface. Given the major CH_4 source distributions in East Asia, the strong northward air flow along the coast could reduce local CH_4 accumulation, but transport the CH_4-rich air effectively to the north and then to Japan as turning around the Korean peninsula. In September 2013, the wind speed over Japan was much lower than August, but wind still blows westerly from the continent to Japan. This slower westerly air flow could maintain the higher level of XCH_4 over Japan during the September of 2013.

The wind patterns we examined above shows us how the atmospheric transport field in 2013 differed from a climatological field on a regional-scale. In order to narrow down the origins and the upstream patterns of the air masses to the Japanese TCCON sites, we conducted back trajectory analysis using the Stochastic Time-Inverted Lagrangian Transport (STILT) model (Lin et al., 2003), driven by Global Data Assimilation System (GDAS) meteorology (1˚×1˚). To obtain the monthly mean features of the upstream, we released 100 particles from the height of 1500 m (approximately ~850 hPa) at Saga and Tsukuba, at every 12:00 noon local time (= 3 UT) and traveled backward for 10-days. Every 30 minutes, the number of particles was counted by a 1˚×1˚ air column and the total number of particles over the 10 day duration was divided by the maximum number per column. Thus, we obtained a normalized daily upstream pattern and averaged them over a month. Figure 12 shows the monthly normalized trajectories for August and September in 2012 and 2013. There are distinct differences in the upstream patterns between 2012 and 2013. The patterns of the summer of 2012 are almost like climatological; in August, the wind flows dominantly from the Pacific to the Japan, in September the dominant wind direction is in transition; from southeasterly wind (from the Pacific) to northwesterly wind (from the continent). On the other hand, in August 2013 the air masses reached the Japanese TCCON sites from the west, after traveling over the coastal side of East China. In September 2013, the westerly wind from the continent is still dominant, especially for Saga. This backtrajectory result supports that the anomalous wind field in the summer of 2013 brought the CH_4-rich air from China to Japan, resulting in the high XCH_4 observed at the two Japanese TCCON sites and also by GOSAT over Japan.

4.2 Other possible factors

Although we suggest that the atmospheric transport field probably attributes to the enhancement of XCH_4 and CH_4 concentration observed in the summer of 2013, we cannot entirely rule out other possible factors. Here we discuss two factors. One is the surface emission changes. Though the temporal variations in XCH_4 do not necessarily correlate with the surface emissions (e.g., Bloom et al., 2010), the surface emission change is potential to impact on the change in XCH_4. The second is the contribution of stratospheric methane.

The CH_4 emissions from rice cultivations and wetland in Southern China might be enhanced under the hot summer condition in 2013. East Asia around China experienced a hotter summer monsoon season (June-September) by more than 1 ˚C than the season normal (Tokyo Climate Center News No.34 Autumn 2013), while less than 60 % of the normal precipitation in eastern China was reported. A hot weather condition increases the CH_4 emissions through the enhancement of photosynthesis and methanogenic activity in inundated grounds such as wetlands and rice paddies; while a dry condition reduces the CH_4 emissions from wetlands as the water table levels in the ground become low. Thus, the hot and dry weather conditions have opposite effects on the CH_4 emissions from wetlands. The time delay in the correlation between CH_4 emissions and climate anomalies should be considered as the groundwater plays an important role in wetland CH_4 emissions. Furthermore, since rice cultivation is human-managed, multiple controlling factors on CH_4 emissions from rice paddies should be considered. A further investigation of wetland and rice CH_4 emission changes responding to the climate anomaly in East Asia is needed.

Another possibility is the contribution of stratospheric methane. Saad et al. (2014) presented the analysis that the stratospheric methane causes short-term fractionations in total column averaged CH_4 observed at several TCCON sites. The contribution of stratospheric methane to the anomaly in summer 2013 is supposed to be minor or less influential. Firstly the surface CH_4 concentrations at COI and RYO increased in August 2013 when the XCH_4 anomaly occurred, suggesting the major contributor on the anomaly is in the troposphere. Secondly, the order of the stratospheric methane fractionation is smaller than ~3 ppb, which would not be enough to produce the anomaly of an order of ~20 ppb.

5 Conclusion

In this study, we have examined the ~~synoptic-scale~~ extremely high XCH_4 event over Northeast Asia observed by GOSAT in August and September, 2013. Similar XCH_4 enhancements in amplitude and timing were observed at the two Japanese TCCON sites, Tsukuba and Saga. Furthermore, during the same period, the ground-based atmospheric CH_4 monitoring sites of Ryori and Ochi-ishi located in the northern part of Japan observed the higher levels of surface CH_4. In particular, surface CH_4 concentrations at Ryori showed the rapid increase in the middle of August 2013.

Our model analysis indicates that the significant enhancement of XCH_4 and surface CH_4 are mainly attributed to the anomalous atmospheric pressure patterns of Pacific High and Tibetan High over East Asia during the summer of 2013. The CH_4-rich air was effectively ~~was~~ transported to Japan from the major CH_4 source area in East China. The model analysis also indicates that the XCH_4 enhancement occurred in a limited area of the northeastern China to the Japan main island. The two Japanese TCCON sites, ~1,000 km apart from each other, happened to be located along the anomalously CH_4-rich air flow from the Eurasian continent, and coincidentally observed the extreme increase of XCH_4. The GOSAT ~~orbiting~~ with three-day recurrence successfully observed the high XCH_4 event. This data analysis study demonstrates the capability of ~~space-based observation by~~ GOSAT to monitor ~~an~~ the synoptic-scale XCH_4 event ~~of XCH_4 event on a synoptic scale~~ in the association with the high-pressure system anomalies in the comparable accuracy with ground-based observations. The GOSAT capability to detect synoptic variations could be helpful to quantify the relative contribution of atmospheric transport, leading to better estimation of regional CH_4 fluxes.

Acknowledgements

Surface CH_4 data observed at Ryori and Yonagunijima are got from the WDCGG (http://ds.data.jma.go.jp/gmd/wdcgg/). TCCON data were obtained from the TCCON Data Archive, operated by the California Institute of Technology from the website at tccon.ipac.caltech.edu.

References

Alexe, M., Bergamaschi, P., Segers, A., Detmers, R., Butz, A., Hasekamp, O., Guerlet, S., Parker, R., Boesch, H., Frankenberg, C., Scheepmaker, R. A., Dlugokencky, E., Sweeney, C., Wofsy, S. C., and Kort, E. A.: Inverse modelling of CH_4 emissions for 2010–2011 using different satellite retrieval products from GOSAT and SCIAMACHY, Atmos. Chem. Phys., 15, 113-133, 10.5194/acp-15-113-2015, 2015.

Belikov, D. A., Maksyutov, S., Sherlock, V., Aoki, S., Deutscher, N. M., Dohe, S., Griffith, D., Kyro, E., Morino, I., Nakazawa, T., Notholt, J., Rettinger, M., Schneider, M., Sussmann, R., Toon, G. C., Wennberg, P. O., and Wunch, D.: Simulations of column-averaged CO_2 and CH_4 using the NIES TM with a hybrid sigma-isentropic (σ-θ) vertical coordinate, Atmos. Chem. Phys., 13, 1713-1732, 10.5194/acp-13-1713-2013, 2013.

Bergamaschi, P., Frankenberg, C., Meirink, J. F., Krol, M., Dentener, F., Wagner, T., Platt, U., Kaplan, J. O., Körner, S., Heimann, M., Dlugokencky, E. J., and Goede, A.: Satellite chartography of atmospheric methane from SCIAMACHY on board ENVISAT: 2. Evaluation based on inverse model simulations, J. Geophys. Res., 112, 10.1029/2006JD007268, 2007.

Bergamaschi, P., Frankenberg, C., Meirink, J. F., Krol, M., Villani, M. G., Houweling, S., Dentener, F., Dlugokencky, E. J., Miller, J. B., Gatti, L. V., Engel, A., and Levin, I.: Inverse modeling of global and regional CH_4 emissions using SCIAMACHY satellite retrievals, J. Geophys. Res., 114, 10.1029/2009jd012287, 2009.

Bergamaschi, P., Krol, M., Meirink, J. F., Dentener, F., Segers, A., van Aardenne, J., Monni, S., Vermeulen, A. T., Schmidt, M., Ramonet, M., Yver, C., Meinhardt, F., Nisbet, E. G., Fisher, R. E., O'Doherty, S., and Dlugokencky, E. J.: Inverse modeling of European CH_4 emissions 2001–2006, J. Geophys. Res., 115, D22309, 10.1029/2010JD014180, 2010.

Bergamaschi, P., Houweling, S., Segers, A., Krol, M., Frankenberg, C., Scheepmaker, R. A., Dlugokencky, E., Wofsy, S. C., Kort, E. A., Sweeney, C., Schuck, T., Brenninkmeijer, C., Chen, H., Beck, V., and Gerbig, C.: Atmospheric CH_4 in the first decade of the 21st century: Inverse modeling analysis using SCIAMACHY satellite retrievals and NOAA surface measurements, J. Geophys. Res., 118, 7350-7369, 10.1002/jgrd.50480, 2013.

Bloom, A. A., Palmer, P. I., Fraser, A., Reay, D. S., and Frankenberg, C.: Large-Scale Controls of Methanogenesis Inferred from Methane and Gravity Spaceborne Data, Science, 327, 322-325, 10.1126/science.1175176, 2010.

Bousquet, P., Ciais, P., Miller, J. B., Dlugokencky, E. J., Hauglustaine, D. A., Prigent, C., Van der Werf, G. R., Peylin, P., Brunke, E. G., Carouge, C., Langenfelds, R. L., Lathiere, J., Papa, F., Ramonet, M., Schmidt, M., Steele, L. P., Tyler, S. C., and White, J.: Contribution of anthropogenic and natural sources to atmospheric methane variability, Nature, 443, 439-443, 10.1038/nature05132, 2006.

Cressot, C., Chevallier, F., Bousquet, P., Crevoisier, C., Dlugokencky, E. J., Fortems-Cheiney, A., Frankenberg, C., Parker, R., Pison, I., Scheepmaker, R. A., Montzka, S. A., Krummel, P. B., Steele, L. P., and Langenfelds, R. L.: On the consistency between global and regional methane emissions inferred from SCIAMACHY, TANSO-FTS, IASI and surface measurements, Atmos. Chem. Phys., 14, 577-592, 10.5194/acp-14-577-2014, 2014.

Crevoisier, C., Nobileau, D., Fiore, A. M., Armante, R., Chédin, A., and Scott, N. A.: Tropospheric methane in the tropics – first year from IASI hyperspectral infrared observations, Atmos. Chem. Phys., 9, 6337-6350, 10.5194/acp-9-6337-2009, 2009.

Dee, D. P., Uppala, S. M., Simmons, A. J., Berrisford, P., Poli, P., Kobayashi, S., Andrae, U., Balmaseda, M. A., Balsamo, G., Bauer, P., Bechtold, P., Beljaars, A. C. M., van de Berg, L., Bidlot, J., Bormann, N., Delsol, C., Dragani, R., Fuentes, M., Geer, A. J., Haimberger, L., Healy, S. B., Hersbach, H., Hólm, E. V., Isaksen, L., Kållberg, P., Köhler, M., Matricardi, M., McNally, A. P., Monge-Sanz, B. M., Morcrette, J. J., Park, B. K., Peubey, C., de Rosnay, P., Tavolato, C., Thépaut, J. N., and Vitart, F.: The ERA-Interim reanalysis: configuration and performance of the data assimilation system, Q. J. R. Meteorolog. Soc., 137, 553-597, 10.1002/qj.828, 2011.

Dlugokencky, E. J., Bruhwiler, L., White, J. W. C., Emmons, L. K., Novelli, P. C., Montzka, S. A., Masarie, K. A., Lang, P. M., Crotwell, A. M., Miller, J. B., and Gatti, L. V.: Observational constraints on recent increases in the atmospheric CH_4 burden, Geophys. Res. Lett., 36, L18803, 10.1029/2009GL039780, 2009.

Etheridge, D. M., Steele, L. P., Francey, R. J., and Langenfelds, R. L.: Atmospheric methane between 1000 A.D. and present: Evidence of anthropogenic emissions and climatic variability, J. Geophys. Res., 103, 15979-15993, 10.1029/98JD00923, 1998.

Forster, P., Ramaswamy, V., Artaxo, P., Berntsen, T., Betts, R., Fahey, D. W., Haywood, J., Lean, J., Lowe, D. C., Myhre, G., Nganga, J., Prinn, R., Raga, G., Schulz, M., and Van Dorland, R.: Changes in atmospheric constituents and in radiative forcing, in: Climate Change 2007: The Physical Science Basis. Contribution of Working Group I to the Fourth Assessment Report of the Intergovernmental Panel on Climate Change, edited by: Solomon, S., Qin, D., Manning, M., Chen, Z., Marquis, Averyt, K. B., Tignor, M., and Miller, H. L., Cambridge University Press, Cambridge, United Kingdom and New York, NY, USA, 129-234, 2007.

Fraser, A., Palmer, P. I., Feng, L., Boesch, H., Cogan, A., Parker, R., Dlugokencky, E. J., Fraser, P. J., Krummel, P. B., Langenfelds, R. L., O'Doherty, S., Prinn, R. G., Steele, L. P., van der Schoot, M., and Weiss, R. F.: Estimating regional methane surface fluxes: the relative importance of surface and GOSAT mole fraction measurements, Atmos. Chem. Phys., 13, 5697-5713, 10.5194/acp-13-5697-2013, 2013.

Fung, I., John, J., Lerner, J., Matthews, E., Prather, M., Steele, L. P., and Fraser, P. J.: Three-dimensional model synthesis of the global methane cycle, J. Geophys. Res., 96, 13033-13065, 10.1029/91JD01247, 1991.

Hansen, J., and Sato, M.: Greenhouse gas growth rates, Proc. Natl. Acad. Sci. U.S.A., 101, 16109-16114, 10.1073/pnas.0406982101, 2004.

Ito, A., and Inatomi, M.: Use of a process-based model for assessing the methane budgets of global terrestrial ecosystems and evaluation of uncertainty, Biogeosciences, 9, 759-773, 10.5194/bg-9-759-2012, 2012.

Houweling, S., Krol, M., Bergamaschi, P., Frankenberg, C., Dlugokencky, E. J., Morino, I., Notholt, J., Sherlock, V., Wunch, D., Beck, V., Gerbig, C., Chen, H., Kort, E. A., Röckmann, T., and Aben, I.: A multi-year methane inversion using SCIAMACHY, accounting for systematic errors using TCCON measurements, Atmos. Chem. Phys., 14, 3991-4012, 10.5194/acp-14-3991-2014, 2014.

Kirschke, S., Bousquet, P., Ciais, P., Saunois, M., Canadell, J. G., Dlugokencky, E. J., Bergamaschi, P., Bergmann, D., Blake, D. R., Bruhwiler, L., Cameron-Smith, P., Castaldi, S., Chevallier, F., Feng, L., Fraser, A., Heimann, M., Hodson, E. L., Houweling, S., Josse, B., Fraser, P. J., Krummel, P. B., Lamarque, J.-F., Langenfelds, R. L., Le Quéré, C., Naik, V., O'Doherty, S., Palmer, P. I., Pison, I., Plummer, D., Poulter, B., Prinn, R. G., Rigby, M., Ringeval, B., Santini, M., Schmidt, M., Shindell, D. T., Simpson, I. J., Spahni, R., Steele, L. P., Strode, S. A., Sudo, K., Szopa, S., van der Werf, G. R., Voulgarakis, A., van Weele, M., Weiss, R. F., Williams, J. E., and Zeng, G.: Three decades of global methane sources and sinks, Nat. Geosci., 6, 813-823, 10.1038/ngeo1955, 2013.

Kort, E. A., Frankenberg, C., Costigan, K. R., Lindenmaier, R., Dubey, M. K., and Wunch, D.: Four corners: The largest US methane anomaly viewed from space, Geophys. Res. Lett., 41, 2014GL061503, 10.1002/2014GL061503, 2014.

Kuze, A., Suto, H., Nakajima, M., and Hamazaki, T.: Thermal and near infrared sensor for carbon observation Fourier-transform spectrometer on the Greenhouse Gases Observing Satellite for greenhouse gases monitoring, Appl. Opt., 48, 6716-6733, 10.1364/AO.48.006716, 2009.

Lin, J. C., Gerbig, C., Wofsy, S. C., Andrews, A. E., Daube, B. C., Davis, K. J., and Grainger, C. A.: A near-field tool for simulating the upstream influence of atmospheric observations: The Stochastic Time-Inverted Lagrangian Transport (STILT) model, J. Geophys. Res.-Atmos., 108, Doi 10.1029/2002jd003161, 2003.

Miller, S. M., Wofsy, S. C., Michalak, A. M., Kort, E. A., Andrews, A. E., Biraud, S. C., Dlugokencky, E. J., Eluszkiewicz, J., Fischer, M. L., Janssens-Maenhout, G., Miller, B. R., Miller, J. B., Montzka, S. A., Nehrkorn, T., and Sweeney, C.: Anthropogenic emissions of methane in the United States, Proc. Natl. Acad. Sci. U.S.A., 110, 20018-20022, 10.1073/pnas.1314392110, 2013.

Monteil, G., Houweling, S., Butz, A., Guerlet, S., Schepers, D., Hasekamp, O., Frankenberg, C., Scheepmaker, R., Aben, I., and Röckmann, T.: Comparison of CH4 inversions based on 15 months of GOSAT and SCIAMACHY observations, J. Geophys. Res., 118, 11,807-811,823, 10.1002/2013JD019760, 2013.

Nakazawa, T., Ishizawa, M., Higuchi, K., and Trivett, N. B. A.: Two curve fitting methods applied to CO_2 flask data, Environmtrics, 8, 197-218, 1997.

Onogi, K., Tsutsui, J., Koide, H., Sakamoto, M., Kobayashi, S., Hatsushika, H., Matsumoto, T., Yamazaki, N., Kamahori, H., Takahashi, K., Kadokura, S., Wada, K., Kato, K., Oyama, R., Ose, T., Mannoji, N., and Taira, R.: The JRA-25 Reanalysis, J. Meteor. Soc. Japan, 85, 369-432, 10.2151/jmsj.85.369, 2007.

Patra, P. K., Houweling, S., Krol, M., Bousquet, P., Belikov, D., Bergmann, D., Bian, H., Cameron-Smith, P., Chipperfield, M. P., Corbin, K., Fortems-Cheiney, A., Fraser, A., Gloor, E., Hess, P., Ito, A., Kawa, S. R., Law, R. M., Loh, Z., Maksyutov, S., Meng, L., Palmer, P. I., Prinn, R. G., Rigby, M., Saito, R., and Wilson, C.: TransCom model simulations of CH_4 and related species: linking transport, surface flux and chemical loss with CH_4 variability in the troposphere and lower stratosphere, Atmos. Chem. Phys., 11, 12813-12837, 10.5194/acp-11-12813-2011, 2011.

Saad, K. M., Wunch, D., Toon, G. C., Bernath, P., Boone, C., Connor, B., Deutscher, N. M., Griffith, D. W. T., Kivi, R., Notholt, J., Roehl, C., Schneider, M., Sherlock, V., and Wennberg, P. O.: Derivation of tropospheric methane from TCCON CH_4 and HF total column observations, Atmos. Meas. Tech., 7, 2907-2918, 10.5194/amt-7-2907-2014, 2014.

Schneising, O., Buchwitz, M., Reuter, M., Heymann, J., Bovensmann, H., and Burrows, J. P.: Long-term analysis of carbon dioxide and methane column-averaged mole fractions retrieved from SCIAMACHY, Atmos. Chem. Phys., 11, 2863-2880, 10.5194/acp-11-2863-2011, 2011.

Tanaka, T., Miyamoto, Y., Morino, I., Machida, T., Nagahama, T., Sawa, Y., Matsueda, H., Wunch, D., Kawakami, S., and Uchino, O.: Aircraft measurements of carbon dioxide and methane for the calibration of ground-based high-resolution Fourier Transform Spectrometers and a comparison to GOSAT data measured over Tsukuba and Moshiri, Atmos. Meas. Tech., 5, 2003-2012, 10.5194/amt-5-2003-2012, 2012.

Tohjima, Y., Machida, T., Utiyama, M., Katsumoto, M., Fujinuma, Y., and Maksyutov, S.: Analysis and presentation of in situ atmospheric methane measurements from Cape Ochi-ishi and Hateruma Island, J. Geophys. Res., 107, ACH 8-1-ACH 8-11, 10.1029/2001JD001003, 2002.

Turner, A. J., Jacob, D. J., Wecht, K. J., Maasakkers, J. D., Lundgren, E., Andrews, A. E., Biraud, S. C., Boesch, H., Bowman, K. W., Deutscher, N. M., Dubey, M. K., Griffith, D. W. T., Hase, F., Kuze, A., Notholt, J., Ohyama, H., Parker, R., Payne, V. H., Sussmann, R., Sweeney, C., Velazco, V. A., Warneke, T., Wennberg, P. O., and Wunch, D.: Estimating global and North American methane emissions with high spatial resolution using GOSAT satellite data, Atmos. Chem. Phys., 15, 7049-7069, 10.5194/acp-15-7049-2015, 2015.

van der Werf, G. R., Randerson, J. T., Giglio, L., Collatz, G. J., Mu, M., Kasibhatla, P. S., Morton, D. C., DeFries, R. S., Jin, Y., and van Leeuwen, T. T.: Global fire emissions and the contribution of deforestation, savanna, forest, agricultural, and peat fires (1997–2009), Atmos. Chem. Phys., 10, 11707-11735, 10.5194/acp-10-11707-2010, 2010.

Wecht, K. J., Jacob, D. J., Wofsy, S. C., Kort, E. A., Worden, J. R., Kulawik, S. S., Henze, D. K., Kopacz, M., and Payne, V. H.: Validation of TES methane with HIPPO aircraft observations: Implications for inverse modeling of methane sources, Atmos. Chem. Phys., 12, 1823-1832, 10.5194/acp-12-1823-2012, 2012.

Wecht, K. J., Jacob, D. J., Frankenberg, C., Jiang, Z., and Blake, D. R.: Mapping of North American methane emissions with high spatial resolution by inversion of SCIAMACHY satellite data, J. Geophys. Res., 119, 7741-7756, 10.1002/2014JD021551, 2014.

Wunch, D., Toon, G. C., Wennberg, P. O., Wofsy, S. C., Stephens, B. B., Fischer, M. L., Uchino, O., Abshire, J. B., Bernath, P., Biraud, S. C., Blavier, J. F. L., Boone, C., Bowman, K. P., Browell, E. V., Campos, T., Connor, B. J., Daube, B. C., Deutscher, N. M., Diao, M., Elkins, J. W., Gerbig, C., Gottlieb, E., Griffith, D. W. T., Hurst, D. F., Jiménez, R., Keppel-Aleks, G., Kort, E. A., Macatangay, R., Machida, T., Matsueda, H., Moore, F., Morino, I., Park, S., Robinson, J., Roehl, C. M., Sawa, Y., Sherlock, V., Sweeney, C., Tanaka, T., and Zondlo, M. A.: Calibration of the Total Carbon Column Observing Network using aircraft profile data, Atmos. Meas. Tech., 3, 1351-1362, 10.5194/amt-3-1351-2010, 2010.

Wunch, D., Wennberg, P. O., Toon, G. C., Connor, B. J., Fisher, B., Osterman, G. B., Frankenberg, C., Mandrake, L., O'Dell, C., Ahonen, P., Biraud, S. C., Castano, R., Cressie, N., Crisp, D., Deutscher, N. M., Eldering, A., Fisher, M. L., Griffith, D. W. T., Gunson, M., Heikkinen, P., Keppel-Aleks, G., Kyrö, E., Lindenmaier, R., Macatangay, R., Mendonca, J., Messerschmidt, J., Miller, C. E., Morino, I., Notholt, J., Oyafuso, F. A., Rettinger, M., Robinson, J., Roehl, C. M., Salawitch, R. J., Sherlock, V., Strong, K., Sussmann, R., Tanaka, T., Thompson, D. R., Uchino, O., Warneke, T., and Wofsy, S. C.: A method for evaluating bias in global measurements of CO_2 total columns from space, Atmos. Chem. Phys., 11, 12317-12337, 10.5194/acp-11-12317-2011, 2011.

Yokota, T., Yoshida, Y., Eguchi, N., Ota, Y., Tanaka, T., Watanabe, H., and Maksyutov, S.: Global concentrations of CO_2 and CH_4 retrieved from GOSAT: Frst preliminary results, SOLA, 5, 160-163, 10.2151/sola.2009-041, 2009.

Yoshida, Y., Kikuchi, N., Morino, I., Uchino, O., Oshchepkov, S., Bril, A., Saeki, T., Schutgens, N., Toon, G. C., Wunch, D., Roehl, C. M., Wennberg, P. O., Griffith, D. W. T., Deutscher, N. M., Warneke, T., Notholt, J., Robinson, J., Sherlock, V., Connor, B., Rettinger, M., Sussmann, R., Ahonen, P., Heikkinen, P., Kyrö, E., Mendonca, J., Strong, K., Hase, F., Dohe, S., and Yokota, T.: Improvement of the retrieval algorithm for GOSAT SWIR XCO_2 and XCH_4 and their validation using TCCON data, Atmos. Meas. Tech., 6, 1533-1547, 10.5194/amt-6-1533-2013, 2013.

Figure Captions

Figure 1. Two regions considered in this study: Northeastern China-Korea (115˚E - 130˚E, 30˚N -40˚N, gray-shaded) and Japan (130˚E-145˚E, 30˚N-40˚N, blue-shaded). The locations of the Saga and Tsukuba TCCON stations are marked by closed circles. The open circles are indicated the locations of the surface monitoring stations around Japan, Cape Ochi-ishi (COI), Ryori (RYO), and Yonagunijima (YON).

Figure 2. Temporal variations of GOSAT XCH4 over the two regions of Northeast Asia: (a) Northeastern China – Korea (115˚E-130˚E, 30˚N-40˚N), and (b) Japan (130˚E-145˚E, 30˚N -40˚N). GOSAT XCH4 data are shown in grey dot. The monthly means are plotted in red solid circle and line, whereas monthly means in open circles indicate less than two retrievals available per month. Blue lines indicate the long-term trends. The histogram in the bottom show the number of GOSAT XCH_4 data per month.

Figure 3. Locations of GOSAT soundings with the surface elevations, in the two regions considered in this study. The locations of three capital cities, Tokyo, Seoul and Beijing are also shown in black markers. (a) All soundings of GOSAT data used for 2009-2014. (b) Same with (a) but in August and September 2012. (c) Same with (a) but in August and September 2013.

Figure ~~3~~4. Temporal variations of TCCON XCH4 at (a) Saga (130.29˚E, 33.24˚N) and (b) Tsukuba (140.12˚E, 36.05˚N), Japan. TCCON XCH_4 data are shown in grey dot, daily means in green dots. The monthly means are plotted in red solid circle and line, whereas monthly means in open circles indicate less than two ~~retrievals available~~ observation days per month. Blue lines indicate the long-term trends. The histograms at the bottom show the number of observation day per month.

~~Figure 4.~~ Figure 5. (a) Detrended XCH_4 for 2012 to 2013 at Saga and Tsukuba, Japan and GOSAT over Japan. (b) Same with (a) but also minus mean seasonal cycles. The monthly means of the individual XCH_4 time series are shown in solid lines and circles. The open circles for TCCON indicate that observation days in a month are less than two days. The discontinuity of GOSAT in July 2012 indicates no GOSAT XCH_4 retrieval. Long-term components in individual XCH_4 time series are removed by low pass digital filter of cutoff frequency of two years. Mean seasonal cycles are composed of two harmonics of year and a half year cycles. August and September of both 2012 and 2013 are highlighted.

~~Figure 5.~~ Figure 6. Temporal variations of atmospheric CH_4 concentrations observed at the ground-based monitoring sites around Japan, (a) Cape Ochi-ishi (COI, 43.16˚N, 145.49˚E), (b) Ryori (RYO (39.03˚N, 141.82˚E), and (c) Yonagunijima (YON, 24.47˚N, 123.02˚E). The site locations are shown in Figure 1. Afternoon means of hourly CH4 concentrations are shown in grey lines. The monthly means are plotted in red solid circle and line. Blue lines indicate the long-term trends.

~~Figure 6.~~ Figure 7. Detrended CH4 for 2012 to 2013 at Ryori (RYO) and Cape Ochi-ishi (COI) in Japan. Long-term components in individual CH_4 time series are removed by low pass digital filter of cutoff frequency of two years. August and September of both 2012 and 2013 are highlighted.

~~Figure 7.~~ Figure 8. Spatial distribution of monthly mean modelled (a) CH_4 and (b) XCH_4 in August and September of 2012 and 2013.~~, with respect to surface CH_4 and XCH_4 at South Pole, respectively.~~

Figure 9. Model simulated XCH_4 time-series in comparison with the observed GOSAT XCH_4 over the two target regions of (a) Northeastern China-Korea and (b) Japan, and with the observed TCCON XCH_4 at (c) Saga and (d) Tsukuba. For GOSAT, modeled XCH_4 outputs are sampled at corresponding model grids and averaged by region. August and September of both 2012 and 2013 are highlighted.

Figure 10. Model simulated CH_4 time-series in comparison with the observed CH_4 at (a) Cape Ochi-ishi (COI, 43.16˚N, 145.49˚E), (b) Ryori (RYO (39.03˚N, 141.82˚E), and (c) Yonagunijima (YON, 24.47˚N, 123.02˚E). August and September of both 2012 and 2013 are highlighted.

~~Figure 8.~~ Figure 11. Monthly mean wind fields of August and September at (a) surface and (b) 850hPa. The left panels are the wind fields averaged over the five years of 2009-2013, and the right panels are the monthly mean wind fields of the year 2013.

Figure 12. Monthly mean ten-day backward trajectories from (a) Saga and (b) Tsukuba at 12:00 noon local time (= 3:00 UT). The trajectories started at an altitude of 1500 m (approximately 850 hPa). 100 particles are released every day for a month. To normalize the number density of particles, the particles passed at each 1˚x1˚ grid air column are counted, and the total numbers are divided by the maximum number per grid.

Figure 1

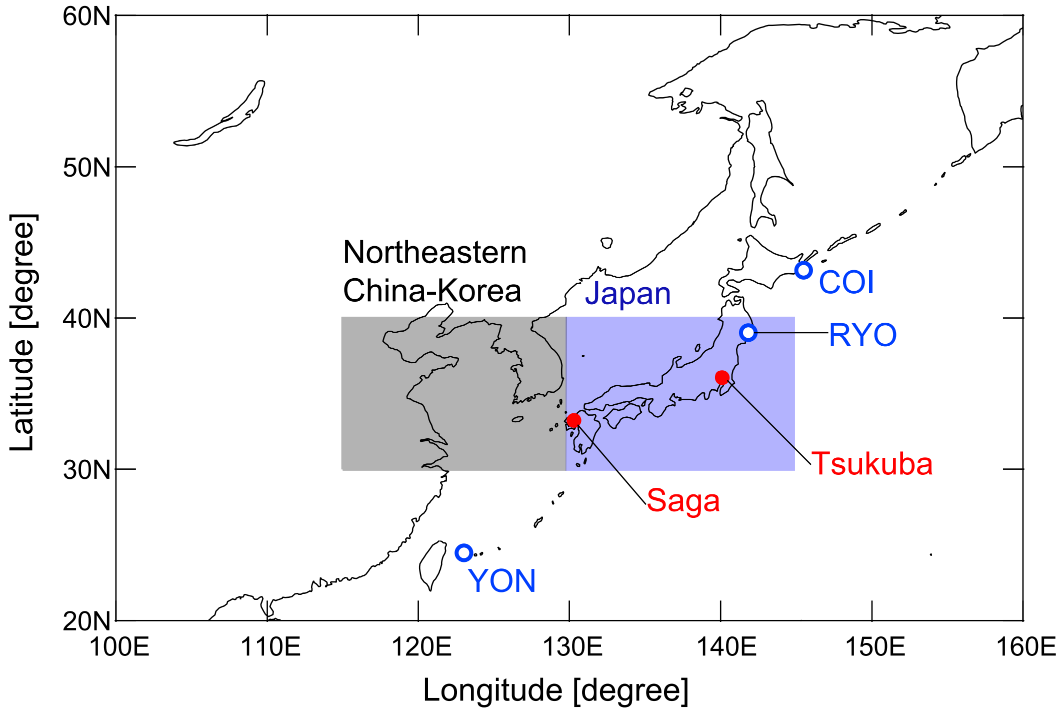

Figure 1. Two regions considered in this study: Northeastern China-Korea (115˚E -130˚E, 30˚N -40˚N, gray-shaded) and Japan (130˚E-145˚E, 30˚N-40˚N, blue-shaded). The locations of the Saga and Tsukuba TCCON stations are marked by closed circles. The open circles are indicated the locations of the surface monitoring stations around Japan, Cape Ochi-ishi (COI), Ryori (RYO), and Yonagunijima (YON).

Figure 2

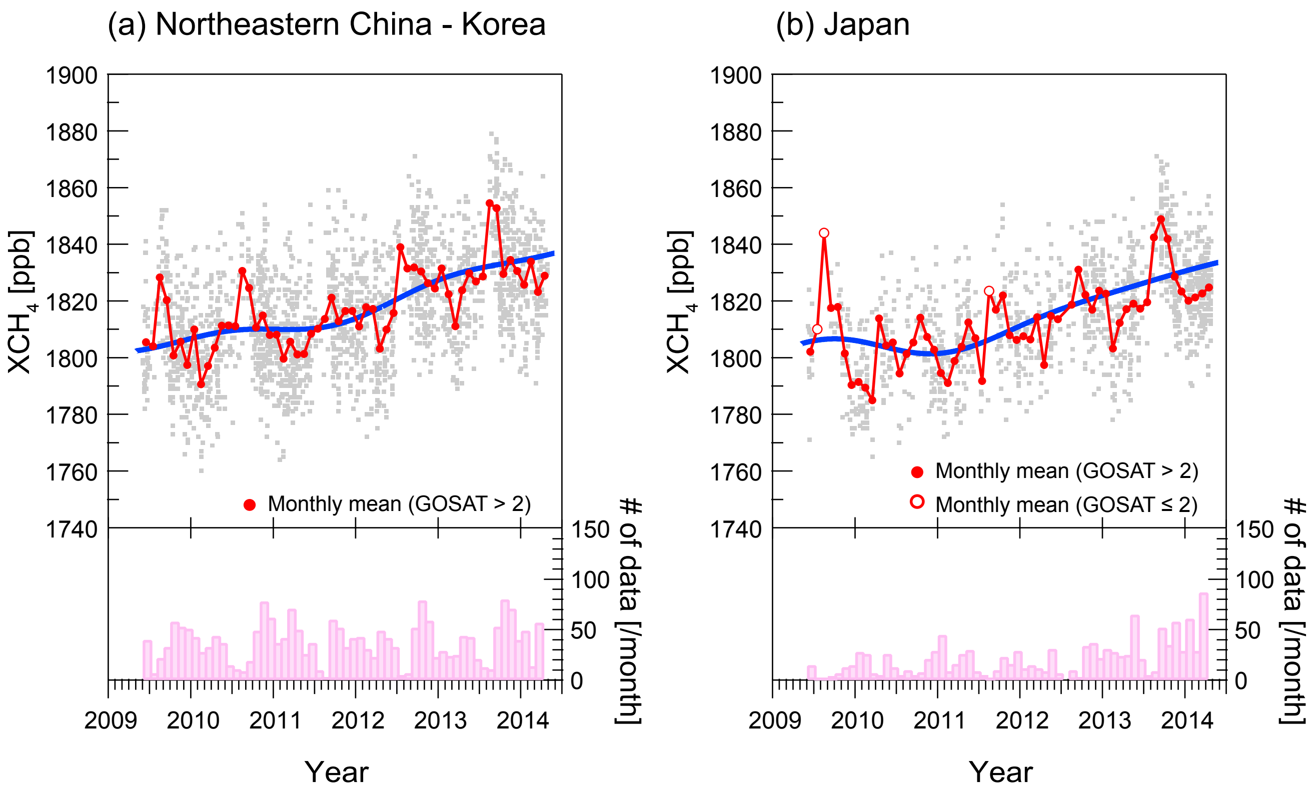

Figure 2. Temporal variations of GOSAT XCH_4 over the two regions of Northeast Asia: (a) Northeastern China – Korea (115˚E-130˚E, 30˚N-40˚N), and (b) Japan (130˚E-145˚E, 30˚N -40˚N). GOSAT XCH_4 data are shown in grey dot. The monthly means are plotted in red solid circle and line, whereas monthly means in open circles indicate less than two retrievals available per month. Blue lines indicate the long-term trends. The histogram in the bottom show the number of GOSAT XCH_4 data per month.

Figure 3

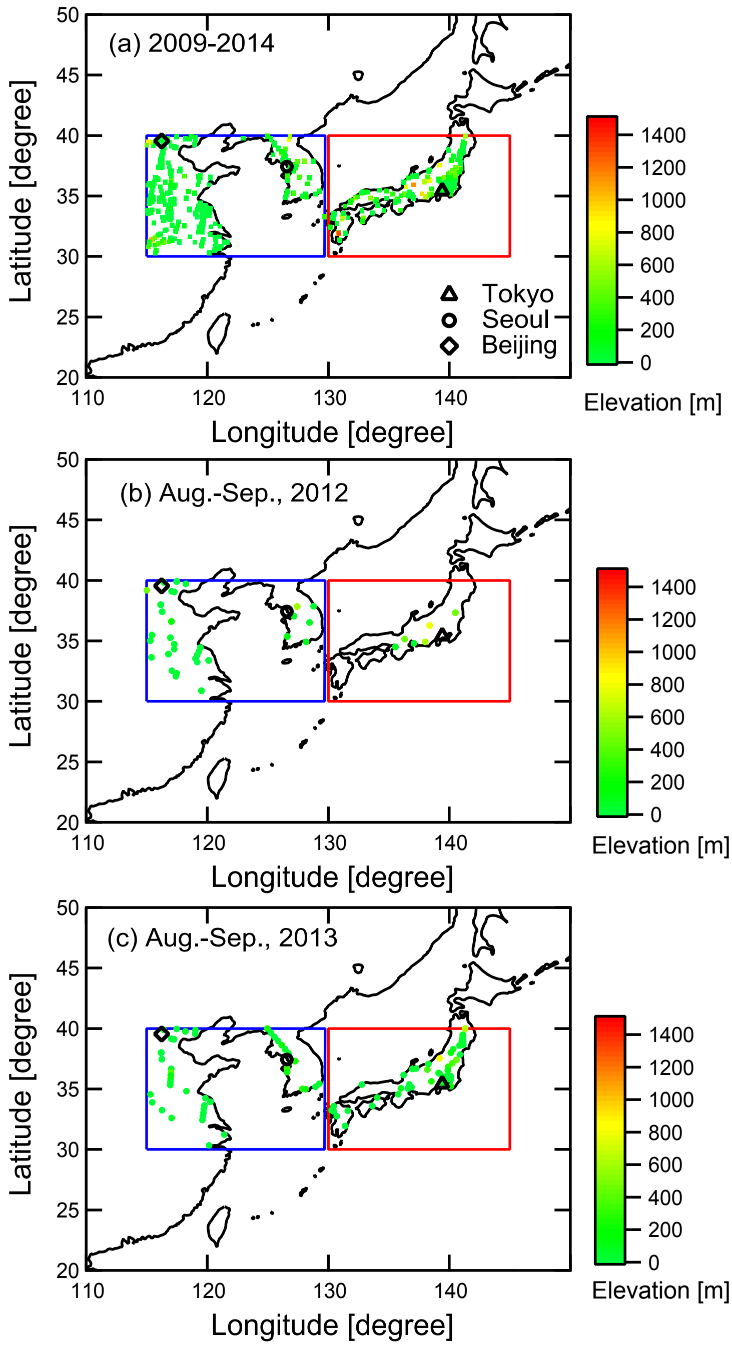

Figure 3. Locations of GOSAT soundings with the surface elevations, in the two regions considered in this study. The locations of three capital cities, Tokyo, Seoul and Beijing are also shown in black markers. (a) All soundings of GOSAT data used for 2009-2014. (b) Same with (a) but in August and September 2012. (c) Same with (a) but in August and September 2013.

Figure 4

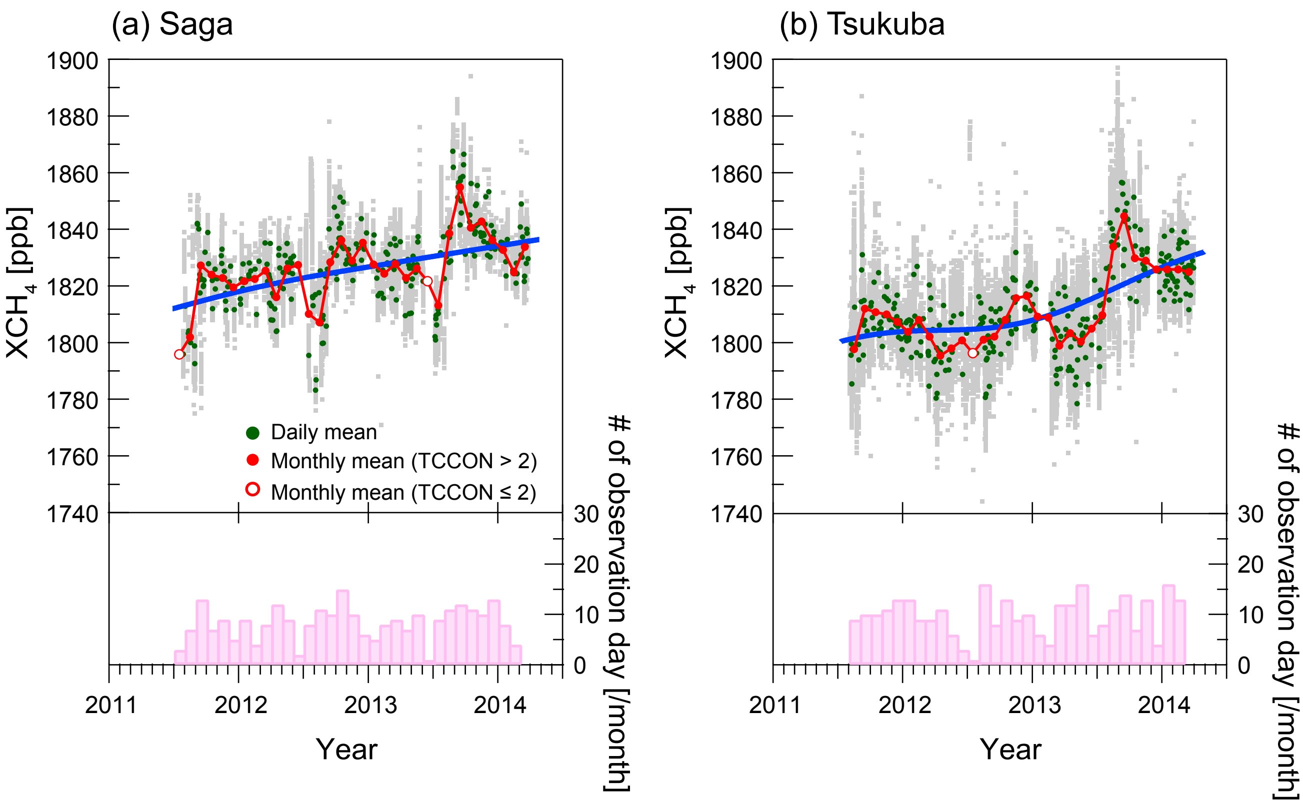

Figure 4. Temporal variations of TCCON XCH_4 at (a) Saga (130.29˚E, 33.24˚N) and (b) Tsukuba (140.12˚E, 36.05˚N), Japan. TCCON XCH_4 data are shown in grey dot, daily means in green dots. The monthly means are plotted in red solid circle and line, whereas monthly means in open circles indicate less than two observation days per month. Blue lines indicate the long-term trends. The histograms at the bottom show the number of observation day per month.

Figure 5.

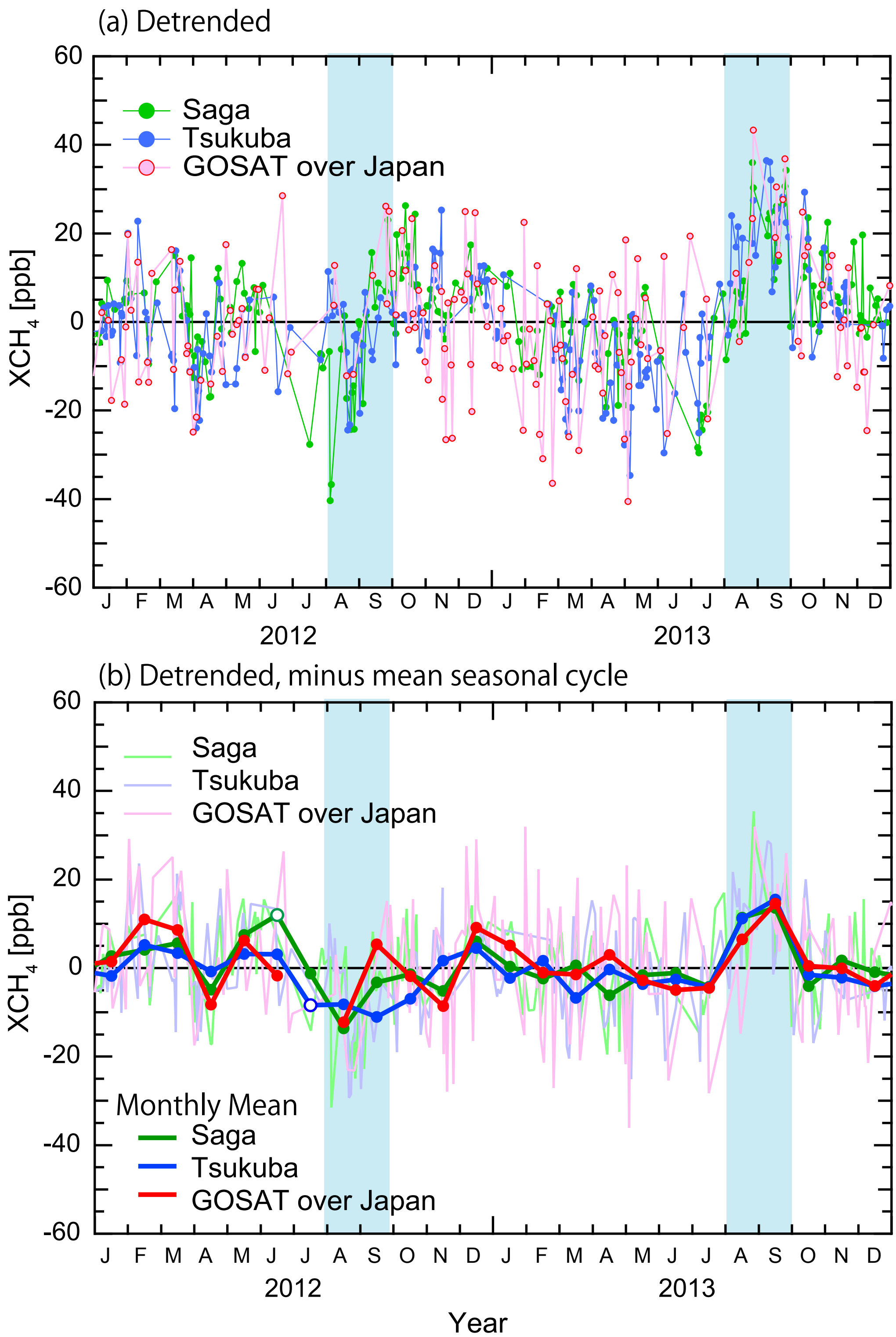

Figure 5. (a) Detrended XCH_4 for 2012 to 2013 at Saga and Tsukuba, Japan and GOSAT over Japan. (b) Same with (a) but also minus mean seasonal cycles. The monthly means of the individual XCH_4 time series are shown in solid lines and circles. The open circles for TCCON indicate that observation days in a month are less than two days. The discontinuity of GOSAT in July 2012 indicates no GOSAT XCH_4 retrieval. Long-term components in individual XCH_4 time series are removed by low pass digital filter of cutoff frequency of two years. Mean seasonal cycles are composed of two harmonics of year and a half year cycles. August and September of both 2012 and 2013 are highlighted.

Figure 6

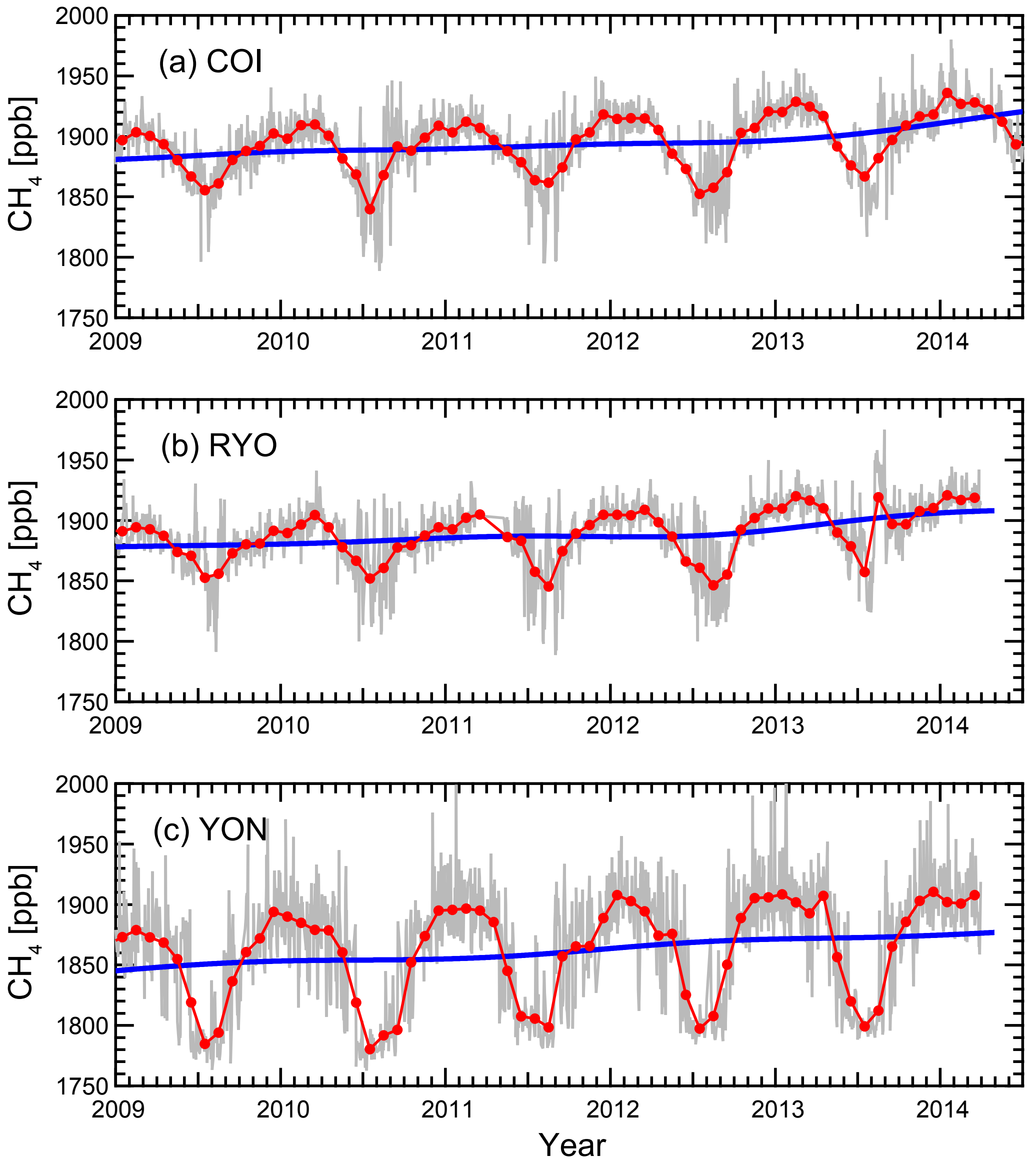

Figure 6. Temporal variations of atmospheric CH_4 concentrations observed at the ground-based monitoring sites around Japan, (a) Cape Ochi-ishi (COI, 43.16˚N, 145.49˚E), (b) Ryori (RYO (39.03˚N, 141.82˚E), and (c) Yonagunijima (YON, 24.47˚N, 123.02˚E). The site locations are shown in Figure 1. Afternoon means of hourly CH_4 concentrations are shown in grey lines. The monthly means are plotted in red solid circle and line. Blue lines indicate the long-term trends.

Figure 7

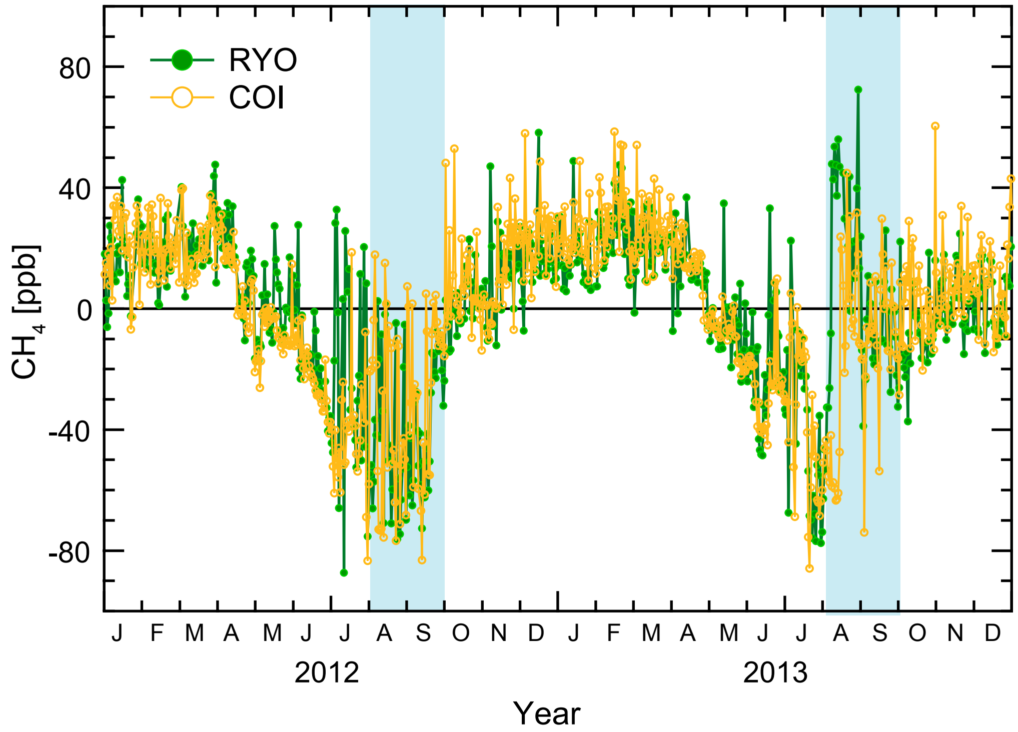

Figure 7. Detrended CH_4 for 2012 to 2013 at Ryori (RYO) and Cape Ochi-ishi (COI) in Japan. Long-term components in individual CH_4 time series are removed by low pass digital filter of cutoff frequency of two years. August and September of both 2012 and 2013 are highlighted.

Figure 8

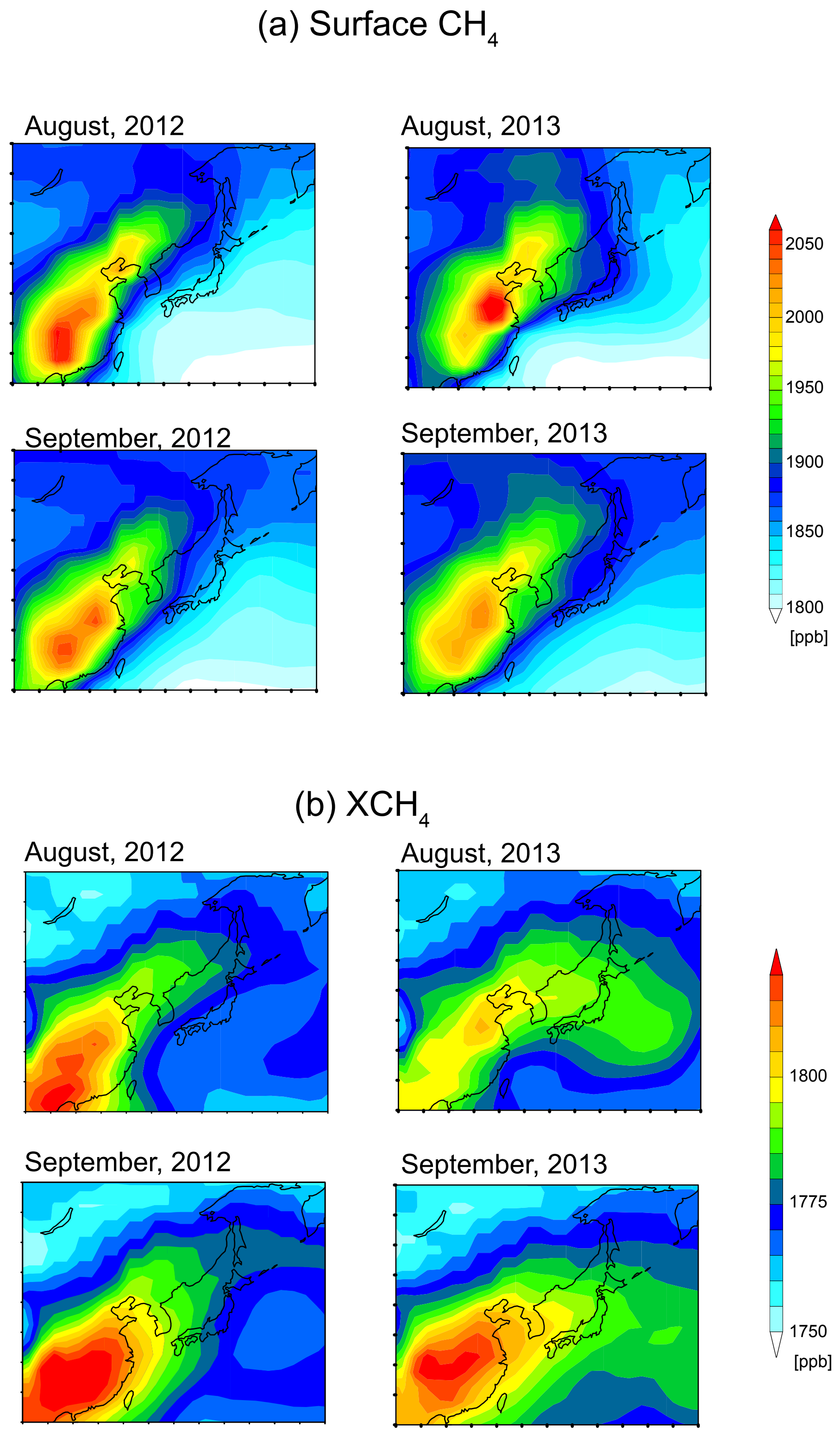

Figure 8. Spatial distribution of monthly mean modelled (a) CH_4 and (b) XCH_4 in August and September of 2012 and 2013.

Figure 9.

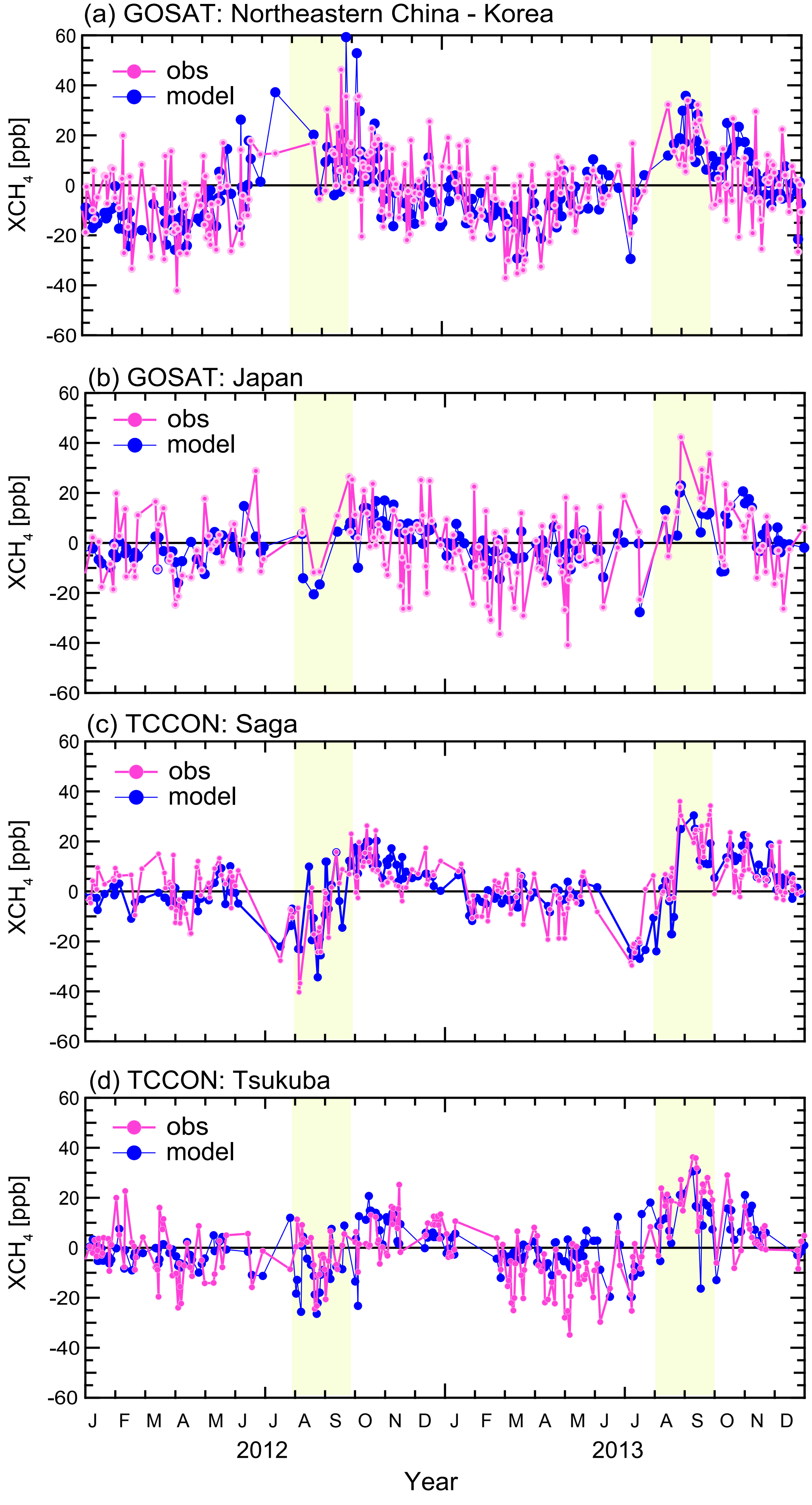

Figure 9. Model simulated XCH_4 time-series in comparison with the observed GOSAT XCH_4 over the two target regions of (a) Northeastern China-Korea and (b) Japan, and with the observed TCCON XCH_4 at (c) Saga and (d) Tsukuba. For GOSAT, modeled XCH_4 outputs are sampled at corresponding model grids and averaged by region. August and September of both 2012 and 2013 are highlighted.

Figure 10

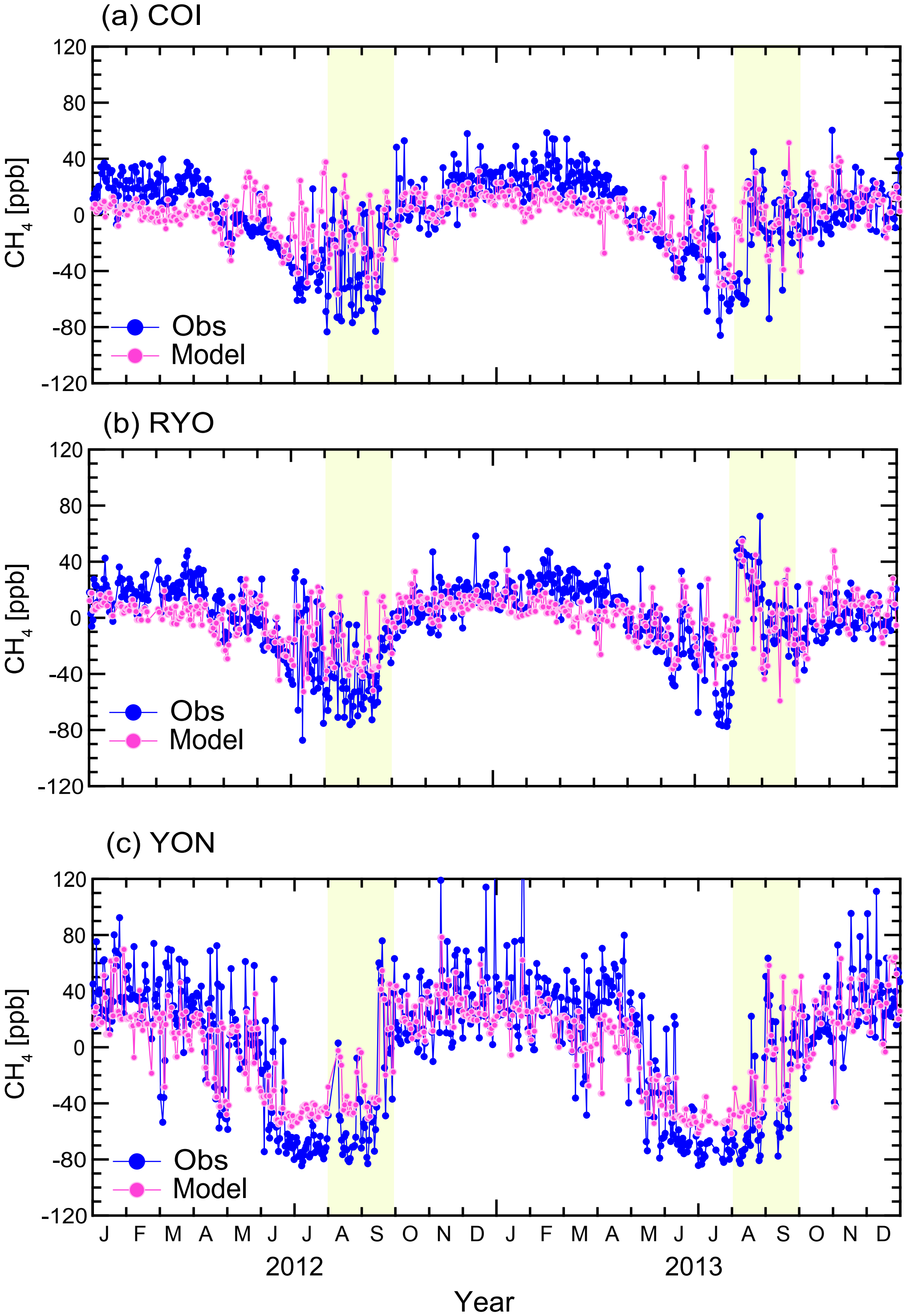

Figure 10. Model simulated CH_4 time-series in comparison with the observed CH_4 at (a) Cape Ochi-ishi (COI, 43.16˚N, 145.49˚E), (b) Ryori (RYO (39.03˚N, 141.82˚E), and (c) Yonagunijima (YON, 24.47˚N, 123.02˚E). August and September of both 2012 and 2013 are highlighted.

Figure 11

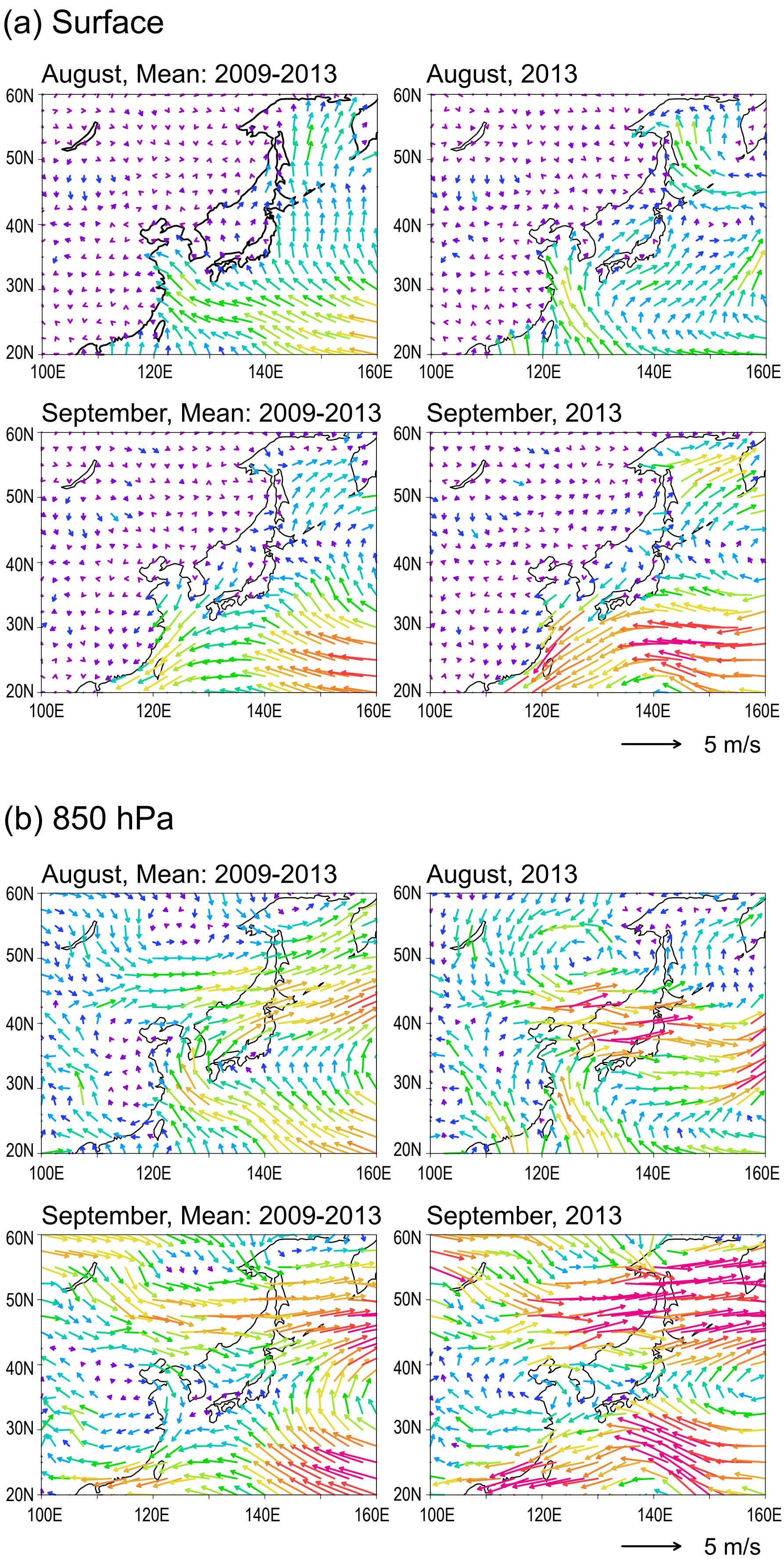

Figure 11. Monthly mean wind fields of August and September at (a) surface and (b) 850hPa. The left panels are the wind fields averaged over the five years of 2009-2013, and the right panels are the monthly mean wind fields of the year 2013.

Figure 12.

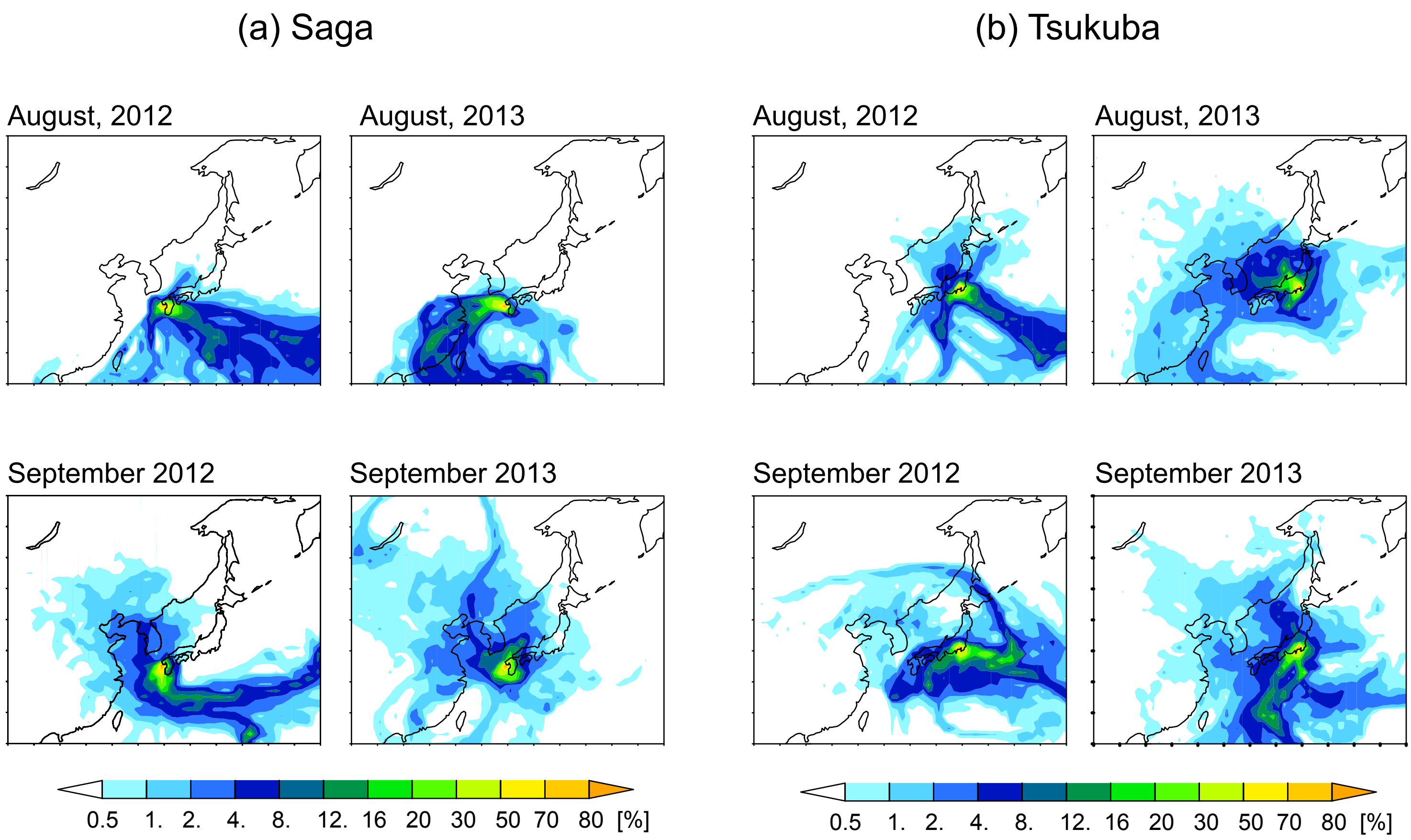

Figure 12. Monthly mean ten-day backward trajectories from (a) Saga and (b) Tsukuba at 12:00 noon local time (= 3:00 UT). The trajectories started at an altitude of 1500 m (approximately 850 hPa). 100 particles are released every day for a month. To normalize the number density of particles, the particles passed at each 1˚x1˚ grid air column are counted, and the total numbers are divided by the maximum number per grid.